ELECTRORECEPTION IN CARCHARHINID AND SPHYRNID SHARKS

A DISSERTATION SUBMITTED TO THE GRADUATE DIVISION OF THE UNIVERSITY OF HAWAI‘I IN PARTIAL FULFILLMENT OF THE REQUIREMENTS FOR THE DEGREE OF

DOCTOR OF PHILOSOPHY

IN

ZOOLOGY

DECEMBER 2001

By
Stephen M. Kajiura

Dissertation Committee:

Kim N. Holland, Chairman
David W. Greenfield
George S. Losey
Ernst S. Reese
Frank T. Koide
John G. Learned

We certify that we have read this dissertation and that, in our opinion, it is satisfactory in scope and quality as a dissertation for the degree of Doctor of Philosophy in Zoology.

DISSERTATION COMMITTEE

_____
Chairperson

_____

_____

_____

_____

_____

ACKNOWLEDGEMENTS

Any dissertation is not the work of an individual but the collaborative effort of many. I thank primarily my committee members, Dave Greenfield, George Losey, Ernie Reese, Frank Koide and John Learned, each of whom contributed significantly to the development of this dissertation. I especially thank my committee chairperson, Kim Holland, for his insight, support and patience with me during my long tenure in his lab. All of my labmates throughout the years provided support in many ways. I thank Aaron Bush, Kanesa Duncan, Tim Fitzgerald, Chris Lowe, Carl Meyer and Brad Wetherbee for their discussions, guidance, assistance, friendship and moral support. Special thanks are extended to Tim Fitzgerald for his ready assistance with long line fishing for sandbar sharks and help with measuring electric fields in seawater.

Head samples from various shark species were provided by several individuals. I thank Aaron Bush and Ricky Chan for scalloped hammerhead shark samples, Doug Adams, Charlie Manire, John Tyminski and Forrest Young for bonnethead shark samples and Wes Pratt and Brad Wetherbee for sandbar shark samples. It is always a tragedy when an elasmobranch dies, and the greatest tragedy is when we as scientists are in some way responsible for the death of the organisms we study. No sharks were deliberately killed for this study; every head sample I received was from an incidental mortality.

I was dependent on the goodwill of many other people who helped with various aspects of the research. I thank Bo Alexander, Johnoel Ancheta, Kim Andrews, Jerry Crow, Dean Grubbs, Dave Itano, Dave Kahue, Filiesha LeRand, Charles Longway,

Aaron & Virginia Moriwake, Peter Nelson, Richard Nordman and Tim Tricas for their contributions to this dissertation. Filiesha LeRand was instrumental in care and feeding of the sharks and Dave Kahue deserves special mention for the many hours he spent in the water assisting with the behavioral experiments. I am particularly gratefully to Tim Tricas for patiently teaching me about electroreception and always being willing to help me to understand.

Financial support was provided by grants from the Raney Fund for Ichthyological Research, the Hawaii Institute of Marine Biology Student Travel Fund, the Sandina L. Lord Scholarship and the University of Hawaii Graduate Student Organization.

ABSTRACT

The evolution of the unique head morphology of hammerhead sharks (Family Sphyrnidae) has been the subject of much speculation. The dorso-ventrally compressed and laterally expanded pre-branchial head forms a cephalofoil that is an unmistakable diagnostic feature of the sphyrnid sharks. Various hypotheses have been advanced to explain the adaptive significance of this peculiar head morphology but few have been empirically tested. This study tests one specific hypothesis, the enhanced electrosensory hypothesis, to determine if the sphyrnid head morphology confers an electrosensory advantage compared to the pointed-snout head morphology typical of their close relatives, the carcharhinid sharks. Scalloped hammerhead sharks, Sphyrna lewini, have a greater head width than similar sized sandbar sharks, Carcharhinus plumbeus, and also have a greater number of electrosensory pores (3068.3±26.7SE vs. 2317.3±26.3SE). The greater number of electrosensory pores are distributed over a greater surface area thus providing the hammerhead cephalofoil with a pore density (pores cm^{-2}) equivalent to that of similar sized sandbar sharks. Despite gross differences in head morphology, the general distribution pattern of pores is conserved on both species. Both species orient to and bite at prey-simulating dipole electric fields in the seawater. The minimum electric field intensities at which the sharks initiate an orientation toward the dipole (i.e., response threshold) are similar for both species (S. lewini: median = 25.2 nV cm^{-1}, minimum < 1nV cm^{-1}; C. plumbeus: median = 30.3 nV cm^{-1}, minimum < 1nV cm^{-1}). Therefore, the hammerheads do not demonstrate greater sensitivity to electric fields than the sandbar sharks. The smaller cross sectional area of the trunk of the hammerheads enables them to

exhibit a greater degree of flexibility that is manifest in a greater repertoire of orientation pathways compared to the sandbar sharks. The greater head width of the hammerheads enables them to sample a greater area with equivalent resolution to the smaller area sampled by the head of similar sized sandbar sharks. Therefore, although the hammerheads are not more sensitive than the sandbar sharks to prey-simulating dipole electric fields, their wider head does provide them with a greater probability of prey encounter. Thus, the enhanced electrosensory hypothesis is supported as an explanation of the adaptive significance of the sphyrnid cephalofoil.

TABLE OF CONTENTS

LIST OF TABLES

LIST OF FIGURES

CHAPTER 1

INTRODUCTION TO ELASMOBRANCH ELECTRORECEPTION

INTRODUCTION

Any morphological change from a basal form is subjected to natural selection and must not be detrimental if it is to be maintained. A morphologically extreme deviation must confer benefits that outweigh the costs. The peculiar head morphology of hammerhead sharks represents an example of an extreme morphological deviation from a basal form. The eight species of hammerhead shark (Family Sphyrnidae) are characterized by a head morphology that is not present in any other extant vertebrate. The dorso-ventrally compressed and laterally expanded pre-branchial head is an unmistakable distinguishing feature of the sphyrnid sharks. This unique head morphology has been termed the "cephalofoil" in recognition of its wing-like appearance (Compagno 1984).

The persistence of the sphyrnid cephalofoil over the past 20 to 25 million years (Cappetta 1987) and the accompanying radiation into several hammerhead species of various head morphologies (Gilbert 1967) tell of its evolutionary success. Several hypotheses have been advanced to explain the adaptive significance of the sphyrnid cephalofoil but only a few have been empirically tested. The various hypotheses are not mutually exclusive, but each emphasizes a single selective advantage to justify evolution of the cephalofoil.

Hypotheses

It has been suggested that the cephalofoil evolved from the broad, flattened head typical of many carcharhinid sharks, and acts as a bowplane that provides hydrodynamic lift and increased maneuvering capabilities (Thomson & Simanek 1977; Compagno 1984). The cephalofoil, which theoretically grants the sphyrnids greater anterior lift compared to carcharhinids, simultaneously confers enhanced maneuverability which may aid the sphyrnids in executing sharp turns (Nakaya 1995). A rudder, or canard wing, has greatest effect when placed as far as possible from the center of gravity (Smith 1985). Therefore, the anterior placement of the cephalofoil of sphyrnid sharks will produce the greatest moment thus granting enhanced maneuverability that might enable the sharks to capture fast, agile prey (Nakaya 1995).

Another hypothesis states that the cephalofoil functions in prey manipulation (Strong et al. 1990). This was suggested upon observation of a great hammerhead, Sphyrna mokarran, which used its cephalofoil to batter a stingray to the sea floor and restrain it while the shark bit off the pectoral fins. A carcharhinid shark would be unable to apply pressure across the dorsum of the stingray and would thus not be able to pin the ray while positioning its mouth over the pectoral fins. This specialized function of the cephalofoil however is unlikely to account for the evolution of the extremely wide head morphology of the winghead shark, Eusphyra blochii,or to be advantageous to small sphyrnid species that do not feed on batoids.

Other hypotheses involve potential advantages of spacing sensory structures at the lateral ends of the head or across the surface of the head. It has been suggested that the placement of the nostrils at the distal tips of the cephalofoil may provide sphyrnids with

greater olfactory gradient resolution (Compagno 1984). Bonnethead sharks, S. tiburo, demonstrate olfactory gradient searching by differentially responding to stimuli in one nostril or the other (Johnson & Teeter 1985). However, the increased olfactory resolution hypothesis is not strongly supported upon closer examination of the sphyrnid head morphology. The rostral edge of the cephalofoil of several sphyrnid species is characterized by prenarial grooves that extend up to approximately a third of the head width on each side of the head (Compagno 1984). As the shark swims, water at any point along the rostral edge of the cephalofoil is channeled into the prenarial grooves and transported to the nares. These grooves serve to concentrate the olfactory stimuli at the expense of resolution. That is, there will be an improved ability to determine that an odorant was present but less ability to determine if the source was medial or distal along the rostral edge of the cephalofoil.

Even if the olfactory spatial resolution of sphyrnid sharks does not differ from carcharhinids, there is still the potential for sphyrnids to demonstrate a greater sensitivity to olfactory stimuli. The elongated cephalofoil provides sphyrnids with a nasal capsule that can accommodate larger nasal organs with a greater olfactory epithelial surface area compared to carcharhinids (Compagno 1984). Therefore, sphyrnids have a potentially greater number of sensory cells in contact with the seawater and thus have a greater probability of detecting an odorant.

It has been suggested that the eyes situated at the ends of the cephalofoil might enhance binocular vision anteriorly and increase the lateral visual field in turbid water (Tester 1963). It has also been suggested that the large surface area of the head may

increase the area sampled by the lateral line for prey detection (Compagno 1988). Neither of these hypotheses has been tested.

Finally, by spacing the electrosensory pores across a wide area, the sphyrnid head morphology may provide the sharks with a broader area of coverage and increased probability of encountering the bioelectric fields of prey (Compagno 1984). In addition, the cephalofoil may provide sphyrnids with greater sensitivity and spatial resolution compared to carcharhinid head morphologies (Compango 1988). This is because the length of the electrosensory ampullary tubules is directly proportional to sensitivity (Murray 1974; Bennett & Clusin 1978) and the wider head allows sphyrnids to possess longer ampullary tubules with consequent increased sensitivity to electric fields. Thus, the wider head would sample both a greater volume of the surrounding medium and also could provide greater spatial resolution by detecting differential signal strength across the head. The enhanced electrosensory hypothesis therefore proposes that the sphyrnid head morphology increases probability of prey encounter, increases sensitivity to electric fields and increases spatial resolution of electric stimuli across the head.

In summary, the cephalofoil has been suggested to improve swimming efficiency and maneuverability, aid in prey handling and improve sensory perception. These hypotheses are not mutually exclusive and it is the electroreceptive hypothesis which is investigated in this study.

Electroreception

Electroreception in elasmobranchs is mediated by a sensory system known as the ampullae of Lorenzini. The ampullae of Lorenzini consist of hundreds to thousands of

mucopolysaccharide-filled tubules which extend from pores on the surface of the head of sharks to blind-ending ampullae within the head which are lined with sensory hair cells. The mucopolysaccharide gel is highly conductive with a conductivity almost equal that of seawater (Murray & Potts 1961). In contrast, the cells that compose the walls of the tubules are bound by tight junctions which serve to insulate the gel in the tubules from the surrounding tissues (Waltman 1966). In the presence of an electric gradient, the difference in electric potential from the pore opening on the surface of the head to the base of the sensory hair cells lining the ampulla is directly proportional to the length of the tubule. That is, the longer the tubule, the greater the potential difference along the length and thus, the greater the sensitivity (Murray 1974; Bennett & Clusin 1978). Compare to the walls of the tubules, shark tissue and skin offer a relatively low electrical resistance (Kalmijn 1974) which means that the basal side of the sensory hair cells in the head will be nearly the same potential as the surrounding seawater immediately adjacent to the head. In contrast, the apical side of the hair cells facing the lumen of the ampulla will be at the same potential as the pore opening of the insulated tubule. Thus, the difference in potential across the hair cells is a function of the position of the pore and length of the tubule with respect to the electrical voltage gradient across the head (Figure 1.1).

The ecological function of the ampullae of Lorenzini remained uncertain for many years because electrophysiological experiments demonstrated that the system responded to mechanical pressure (Parker 1909), temperature changes (Sand 1938), salinity changes (Lowenstein & Ishiko 1962), and electrical stimuli (Murray 1960). Behavioral experiments finally determined that the ampullae of Lorenzini act as

electroreceptors which could detect the presence of prey (Kalmijn 1971). All living organisms in seawater generate an electric field around their body which varies in the range from microvolts to millivolts and these natural electric fields are within the range detectable by elasmobranchs (Kalmijn 1972). Surprisingly few studies have addressed the role of electroreception in prey detection or the finer aspects of electrosensory-mediated behavior. Of the few studies that have examined behavioral responses of elasmobranchs to electric fields, none have dealt with sphyrnids, even though it has been hypothesized that their head morphology may have been driven by selection to enhance electroreceptive capabilities (Compagno 1988).

For the more than 380 shark species (Compagno 1999), there are published accounts of electrosensory-mediated prey detection for only eight species in four orders (Table 1.1). The first behavioral study to demonstrate electroreception in a shark involved the spotted dogfish, Scyliorhinus canicula, biting at buried electrodes (Kalmijn 1971). Kalmijn (1982) went on to perform a limited study of pelagic blue sharks, Prionace glauca, and determined that in a two-choice test they preferred to bite at the electrically active dipoles suspended in the water column rather than the non-active control dipoles. A similar experiment yielded comparable results for the white shark, Carcharodon carcharias (Tricas & McCosker 1984). These experiments indicated that electroreception can be utilized by pelagic as well as benthic feeders. Swell sharks, Cephaloscyllium ventriosum, also bite at electric stimuli even in non-bait-attracted situations (Tricas 1982), and nurse sharks can be trained to respond to dipole fields (Johnson et al. 1984). Another elasmobranch that demonstrates a feeding response when presented with an electric field is the electric ray, Torpedo californica (Bray 1978). This

species responds to prey-simulating electric stimuli by discharging its electric organs in an attempt to stun prey.

Table 1.1. Shark species tested for electroreceptive response.

Order	Genus & species	Reference
Squaliformes	Mustelus canis	Kalmijn 1978
Orectolobiformes	Ginglymostoma cirratum	Johnson et al. 1984
Lamniformes	Carcharodon carcharias	Tricas & McCosker 1984
Carcharhiniformes	Scyliorhinus canicula	Kalmijn 1971
	Cephaloscyllium ventriosum	Tricas 1982
	Prionace glauca	Kalmijn 1978
	Triakis semifasciata	Kalmijn 1978
	Negaprion brevirostris	Kalmijn 1978

In addition to the studies of electroreception for prey detection, other studies have examined electroreception as a mechanism for orientation in the earth's magnetic field (Kalmijn 1974; Paulin 1995) and for social (mating-related) interactions (Tricas et al. 1995). It is hypothesized that elasmobranchs can utilize their electroreceptors to detect self-induced electric fields as they swim through the earth's magnetic field (Kalmijn 1974; Paulin 1995). Although there is a theoretical basis for support of this hypothesis, definitive empirical data are lacking. An extension of this hypothesis is that sharks might use their electoreceptors to enable them to orient to geomagnetic anomalies on the sea floor (Klimley 1985). Again, correlative data might support this hypothesis but it remains untested. Elasmobranchs also utilize their electroreceptors for detection of conspecifics for mating (Tricas et al. 1995). Both male and female stingrays orient to

buried females and will also orient to only the bioelectric signature of a conspecific played back through a plastic model (Tricas et al. 1995).

Species comparisons

Most elasmobranch electroreception studies have been conducted on small temperate species and none have compared interspecies differences. Given a sphyrnid and a typical carcharhinid shark of equal lengths, the head of the sphyrnid shark is much wider. Along with greater head width is an increase in length of laterally directed electrosensory tubules (see Chu & Wen 1979). Because sensitivity increases with increasing tubule length, the sphyrnid should be able to detect weaker electric fields than the carcharhinid. In addition, sensitivity is a function of the orientation of the electrosensory tubules with respect to the stimulus. Tubules parallel to a voltage gradient will respond maximally, whereas tubules perpendicular to the gradient will not respond because they are not sampling a change in voltage gradient (Murray 1974). The longest tubules in sphyrnids are directed laterally whereas in carcharhinids they are directed rostro-caudally (see Chu & Wen 1979). It is therefore hypothesized that the angle of orientation to a stimulus will differ for sharks which possess the two head morphologies. Finally, scalloped hammerhead sharks, Sphyrna lewini, have twice as many electrosensory pores as gray reef sharks, Carcharhinus amblyrhynchos (2824 vs. 1440) which may confer greater resolution in prey localization (Daniels 1967).

To test the hypothesis that the cephalofoil provides sphyrnids with greater electrosensory capabilities than carcharhiniform sharks, experiments were conducted on juvenile scalloped hammerhead sharks (S. lewini) and sandbar sharks (Carcharhinus

plumbeus). These species were selected based on convenience of capture and handling, their head morphology, and their feeding ecology. They represent typical sphyrnid and carcharhinid head morphologies and both species are readily available in Kaneohe Bay, Oahu. The feeding ecology of the species is also an important consideration because the sharks were tested for their behavioral response to prey-simulating stimuli. Juvenile scalloped hammerhead and sandbar sharks are both benthic feeders that specialize in small fishes and crustaceans (Clarke 1971; Medved et al. 1985, respectively). Benthic prey often bury themselves in the substratum and are thus invisible and perhaps not easily detected by olfaction or audition. Therefore, it is hypothesized that benthic-feeding sharks might rely on electroreception to localize prey. This study compares feeding behavior between species with comparable diets but different head morphologies.

Experimental outline

To test the hypothesis that the sphyrnid head morphology confers enhanced electrosensory capabilities over the typical carcharhinid head morphology this study examined the response to prey-simulating electric stimuli of two morphologically diverse sharks. This was addressed in three ways.

To test the morphology-based assumptions and predictions of the enhanced electrosensory hypothesis, various head morphometrics were quantified for carcharhinid and sphyrnid sharks. The distribution of electrosensory pores was mapped for the different species and the number of pores was counted and used to calculate the pore density (pores cm^{-2}). These data were used to test the predictions of greater electrosensory resolution in sphyrnid sharks.

To test the behavioral response of sharks to weak electric fields, a stimulus generator circuit was designed that generated prey-simulating electric fields in seawater. The applied stimuli were empirically measured to ensure that the mathematically modeled electric field intensities accurately represented the actual field intensities in the seawater. The response of scalloped hammerhead shark pups, S. lewini, to a range of prey-simulating stimuli was then quantified.

Finally, the responses demonstrated by scalloped hammerhead, S. lewini, and sandbar sharks, C. plumbeus, to prey-simulating stimuli were compared to determine if there were differences in sensitivity or behavior between the two morphologically diverse but similarly sized species.

Thus, this study tested the enhanced electrosensory hypothesis by comparing both morphology and behavior of carcharhinid and sphyrnid sharks to determine if the sphyrnid head morphology confers an electrosensory advantage.

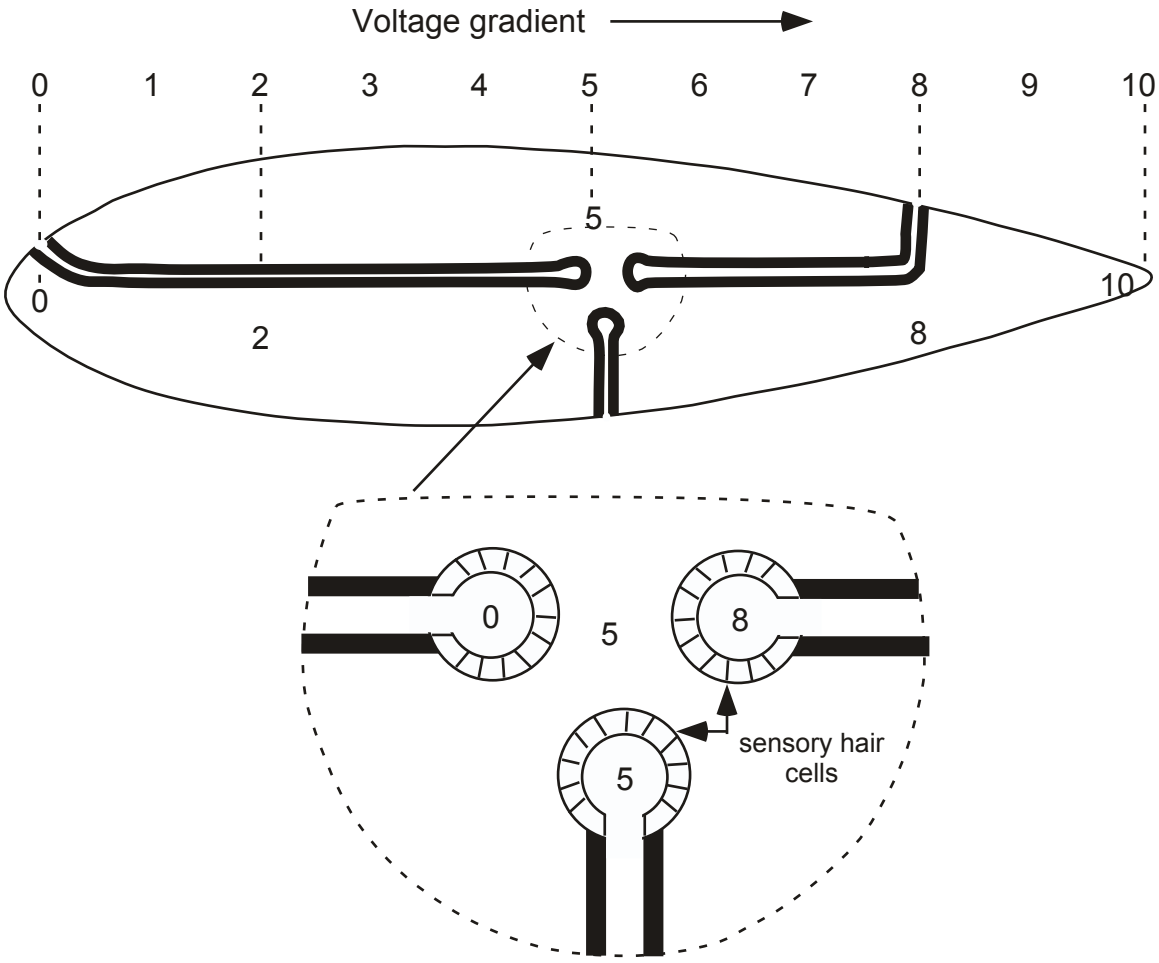

FIGURE 1.1 Diagrammatic representation of a section through a shark head showing the electrosensory canals and ampullae along with the voltage gradient values at various points within the head. The voltage gradient (in arbitrary units) changes with distance across the head. The insulated tubules (thick lines), filled with conductive gel, carry throughout their length the same voltage that exists at the pore opening on the surface of the head. The difference in voltage potential at the base of the ampulla is a function of the length of the tubule and orientation of the tubule with respect to the stimulus voltage gradient. Longer tubules (left) sample a greater voltage change than short tubules (right) or tubules perpendicular to the gradient (bottom). In this example, the difference in potential across the sensory hair cells for the long tubule on the left is 5 units compared to the short tubule on the right where the difference is only 3 units. There is no difference in potential ($\Delta = 0$) for the tubule oriented perpendicular to the gradient. (Modified from Murray 1974).

CHAPTER 2

HEAD MORPHOLOGY AND ELECTROSENSORY PORE DISTRIBUTION OF CARCHARHINID AND SPHYRNID SHARKS

INTRODUCTION

The hammerhead sharks comprise the family Sphyrnidae within the order Carcharhiniformes. They are most closely related to the family Carcharhinidae (Naylor 1992) and share many morphological similarities with carcharhinids; however, they are distinguished from carcharhinids by their unique cephalofoil head morphology.

Several hypotheses have been proposed to explain the evolution of the sphyrnid cephalofoil but few have been empirically tested. The various hypotheses include adaptation to enhance hydrodynamic lift and maneuvering capabilities (Thomson & Simanek 1977; Nakaya 1995), prey handling of batoid elasmobranchs (Strong et al. 1990), greater olfactory gradient resolution (Compagno 1984; Johnson & Teeter 1985), increased visual field (Tester 1963) and increased area for lateral line and electrosensory sampling (Compagno 1984). The various hypotheses are not mutually exclusive and it is the enhanced electrosensory hypothesis that is examined in this study.

The enhanced electrosensory hypothesis states that the laterally expanded sphyrnid cephalofoil maximizes search area coverage to increase the probability of prey detection. The wider head would sample a greater volume of the surrounding medium but there would need to be a corresponding increase in the number of electrosensory pores over the wider head area to maintain comparable spatial resolution of small, prey-generated electric fields. Therefore, the enhanced electrosensory hypothesis assumes that

sphyrnids have a greater head width than comparably sized carcharhinids and predicts that sphyrnids will have a greater number of pores that will yield a comparable or greater pore density.

This study compared the distribution of electrosensory pores on two sphyrnids, the scalloped hammerhead, Sphyrna lewini, the bonnethead, Sphyrna tiburo, and a representative carcharhinid, the sandbar shark, Carcharhinus plumbeus. These species represent a range of head morphologies from the wide hammerhead cephalofoil of S. lewini to the typical carcharhinid head morphology of C. plumbeus with S. tiburo as an intermediate morphology. Various head morphometrics, pore number and pore density were quantified to test the assumption and predictions of the enhanced electrosensory hypothesis.

METHODS

Head morphology

Sharks used were incidental mortalities from other research projects and were collected by gill net or long line fishing. Shark precaudal length (PCL), fork length (FL), total length (TL) and most head morphometrics were measured to the nearest millimeter. Head measurements taken are illustrated in Figure 2.1 and include head width (HW), head length (HL), trunk width (TW), mouth width (MW), mouth length (ML), mouth to snout distance (MS), internarial distance (IN) and left and right head angle (HA). After measurement, heads were severed in the transverse plane at the posterior edge of the lower jaw and the bodies discarded. This position was chosen to standardize shark head

length across species based on a skeletal feature. Also, no electrosensory pores are located caudal to the posterior edge of the lower jaw. Morphometric data were log transformed prior to analysis to allow utilization of linear statistical methods.

The head angle was defined as the angle described by a line from the antero-lateral edge of the incurrent naris to the opposite naris and then to the anterior edge of the center of the head (Figure 2.1). A high-resolution image of the ventral surface of the head was digitized on a flatbed scanner and head angles were measured with image analysis software (NIH Image v1.61). A mean head angle was obtained for each individual by averaging measurements for left and right sides.

Two methods were employed to measure surface area of the head. Each head was placed ventral surface down on a piece of paper and the head outline was traced. The outline was digitized on a flatbed scanner and image analysis software (NIH Image v1.61) was used to measure the area of the head tracing. Surface area was then estimated by doubling the traced area to account for both dorsal and ventral surfaces. A second technique was used to verify the estimate thus obtained. A subsample of ten heads of each species was selected to represent a wide range of sizes. Each head was coated with several coats of liquid latex, which solidifies at room temperature. The latex was removed from the head in quarters (left, right, dorsal, ventral) and each section was laid out, traced, digitized and analyzed as above. From this subsample, a correction factor was generated for each species to more accurately derive the true surface area from the head trace area. Corrected head area data were normalized by log transformation prior to analysis.

Head volume was measured using a seawater volume displacement technique. An acrylic box was filled with seawater to the level of the spillover spigot in the side of the box. A head was placed into the box and the volume of water displaced by the head was measured in a graduated cylinder. Head volume data were log transformed prior to analysis.

After measurement, heads were fixed in 10% formalin, allowed to soak in several changes of freshwater for 24 to 48h, transferred through a graded alcohol series (10%, 20%, 40% isopropanol) and preserved in 40% isopropanol.

Electrosensory pore counts

Total number of electrosensory pores was counted for 35 S. lewini, 19 S. tiburo and 36 C. plumbeus individuals. The size ranges included individuals from juveniles to adults for all species (Table 2.l). Each head was divided into dorsal and ventral surfaces and all pores were counted on both left and right sides. As each pore was counted, fingernail polish was applied with a toothpick to prevent recounting. Four dorsal and eight ventral pore fields were identified based on natural patterns of the pores on the heads (Figures 2.2, 2.3). The pore fields could be recognized on all three species despite the differences in gross morphology of the head. The number of pores in each of the twelve pore fields was examined in a subsample of ten individuals of each species. Counts of left and right sides were summed for each pore field for each individual. A mean number of pores in each pore field was generated for the ten individuals of each species. The percentage of pores in each pore field was calculated from the mean and used to compare the relative number of pores across species.

Table 2.1 Mean number of electrosensory pores, standard deviation, range, sample size and range of shark sizes for scalloped hammerhead, bonnethead and sandbar sharks.

Species	Mean	SD	Range	n	Shark TL (cm)
S. lewini	3068	158.8	2796-3400	35	53.4-247.0
S. tiburo	2028	96.6	1891-2223	19	52.0- 92.0
C. plumbeus	2317	126.3	1983-2585	36	61.6-182.0

To compare the pore distribution patterns, a representative head from each species was selected and the dermis was carefully dissected from the head. The intact dermis was cut along the frontal plane to divide the dermis into dorsal and ventral halves which were cleaned of subdermal tissue. Each dermal sample was sandwiched between panes of glass, backlit by natural sunlight and photographed with color slide film. Pores appeared as bright points of light against a dark background of skin. The photographic slide (35 mm) of each skin sample was projected onto paper, the head outline traced and each pore mapped. This produced a direct one-to-one correspondence map of pores on a head.

RESULTS

Head morphology

The various head morphometrics measured were expressed as percentage of total length and are presented in Table 2.2. The head angle data are not presented in Table 2.2 but are analyzed separately. The head width plotted against the length of the shark for each of the three species is shown in Figure 2.4. A significant interaction effect (non-parallel regression lines for the various species) with the bonnethead shark forced its

exclusion from the analysis of covariance (ANCOVA). However, when the two remaining species were compared, the scalloped hammerhead was demonstrated to have a greater head width than the sandbar shark (ANCOVA, $F_{1,78} = 20.807$, $p < 0.0001$). Even though the bonnethead data could not be statistically tested, it is clear that the bonnetheads were intermediate in head width between the hammerhead and sandbar sharks (Figure 2.4). The head width was approximately 3.02 times the trunk width for S. lewini, 1.68 times the trunk width for S. tiburo and 0.90 times the trunk width for C. plumbeus. Concomitant with the increase in head width was a dramatic decrease in head angle in neonatal S. lewini (Figure 2.5). The anterior head angle of S. lewini decreased by approximately 10° as shark size increased between about 50 to 60 cm TL. This sharp decrease was not seen in C. plumbeus where the slight decline in head angle was linear from neonates to adults. The decrease seen in S. lewini was apparent to a lesser extent in S. tiburo, where the change in head angle was approximately 5°.

Surface area of the heads was compared across the three species (Figure 2.6) as a precursor to calculation of the pore density (pores cm^{-2}). Surface area values estimated by doubling the traced areas were found to underestimate the true surface area of the head for all three species. Values obtained by measuring the latex skins indicated that the trace technique underestimated surface area of the hammerhead by about 1.0%, of the bonnethead by about 6.4% and of the sandbar shark by about 17.1%. Equations were generated to correct the head trace area to a better estimate of the true area based on the latex tracings. The data for the three species were heteroscedastic (non-equivalent variances) so S. tiburo were excluded from the analysis. There was a significant difference in corrected head area between the scalloped hammerhead and the sandbar

shark (ANCOVA, $F_{1,69} = 26.320$, $p < 0.0001$). Although a significant interaction effect existed between the two species, it would be relevant only at total lengths in excess of 5m. As neither species exceeds 3.5m in total length (Compagno 1984), including the results of the ANCOVA was justified. Whereas surface area of the head differed, head volume did not differ significantly between S. lewini and C. plumbeus (ANCOVA, $F_{1,67} = 3.080$, $p = 0.0838$). A significant interaction effect with S. tiburo precluded that species from the volume analysis as well.

Electrosensory pore counts

The scalloped hammerhead, S. lewini, had the greatest number of pores followed by C. plumbeus, and S. tiburo (Table 2.1). The total number of pores did not vary significantly with size (age) of the shark for any of the species (ANOVA, C. plumbeus $F_{1,24} = 0.2160$, $p = 0.6465$; S. tiburo $F_{1,18} = 0.1687$, $p = 0.6864$; S. lewini $F_{1,34} = 0.1290$, $p = 0.7218$). There was no significant difference in number of pores on left and right sides of the head for any species (2 tailed paired t-test, C. plumbeus $t_{24} = 1.7841$, $p = 0.08706$; S. tiburo $t_{18} = 0.6606$, $p = 0.5173$; S. lewini $t_{34} = 0.3446$, $p = 0.7325$). However, the total number of pores differed significantly among all three tested species (ANOVA, $F_{2,76} = 419.9281$, $p < 0.0001$) with S. lewini having more pores than C. plumbeus, which in turn had more pores than S. tiburo (Scheffé, $p < 0.0001$ for all species).

Pore density was calculated as the number of pores cm^{-2}. For all species, pore density was inversely proportional to the size of the shark because pore number remained constant whereas head area increased with shark size (Figure 2.7). Sphyrna lewini juveniles had the greatest pore density with a maximum 18.5 pores cm^{-2}. In contrast, the

maximum pore density achieved by C. plumbeus was 15.7 pores cm^{-2}. Although a significant interaction effect among the species precluded S. tiburo from the analysis, there was no difference in pore density between the scalloped hammerhead and sandbar sharks (ANCOVA, $F_{1,55} = 2.016$, $p = 0.1613$). The greater number of pores in S. lewini combined with the greater surface area provided it with a pore density comparable to that of the sandbar shark. The number of pores on dorsal and ventral surfaces was also compared. The scalloped hammerhead had the greatest number of pores on the ventral surface of the head and yielded a mean dorsal-to-ventral pore ratio of 0.71. The bonnethead had a mean ratio of 0.84. Although both sphyrnid species had a greater number of pores on the ventral surface of the head, C. plumbeus had a distribution of pores close to equal on dorsal and ventral surfaces and yielded a pore ratio of 1.05. Despite the differences in the number of pores on dorsal and ventral surfaces, the general pattern of pore field distribution on the head is conserved across the three examined species (Figures 2.2, 2.3).

The pore distribution pattern on the dorsal surface of the head was divided into four pore fields (Figure 2.2), and the pore distribution pattern on the ventral surface of the head was divided into eight pore fields (Figure 2.3). The percentage of pores in each of the pore fields was mostly comparable among the species (Table 2.3). The notable exceptions included a greater number of pores in section b for the sandbar shark and a greater number of pores in section j for the scalloped hammerhead. In both cases the bonnethead displayed an intermediate value.

DISCUSSION

This study tested the hypothesis that one of the factors that might have driven evolution of the sphyrnid head morphology was an increase in electroreceptive search area (Compagno 1984). If the sphyrnid head morphology was selected to enhance electrosensory prey detection it was assumed that the sphyrnids would possess a laterally expanded head morphology compared to a similar sized carcharhinid. Given a wider head, it was predicted that the sphyrnids would have a greater number of electrosensory pores to maintain a comparable or greater pore density than a carcharhinid. These predictions were supported by the data.

Enhanced electrosensory hypothesis

The assumption of the enhanced electrosensory hypothesis is that the hammerheads have their electroreceptors extended over a greater lateral distance than the carcharhinids. This is obviously true based on the head morphology of the species. Both sphyrnid species have a greater head width than the sandbar shark (Figure 2.4) with electrosensory pores distributed across the entire surface of the head for all species (Figures 2.2, 2.3). Thus, the electroreceptors are distributed over a greater lateral distance in the sphyrnid sharks. One of the factors which drove evolution of the cephalofoil might have been selection for a head in which the electroreceptors were spaced farther apart and thus increased the amount of lateral area sampled by the electrosensory system. This would increase foraging efficiency by allowing the shark to search a larger area of the benthos. For example, a 2m TL sandbar shark has a head

width equivalent to a hammerhead of only 77.9cm TL. Thus, a small hammerhead is able to search the same lateral area as a sandbar shark that is 2.6 times as long.

There is, however, a cost associated with the increased head width of sphyrnid sharks. The broad head, oriented perpendicular to the body axis, makes it potentially difficult for the hammerhead pups to be born. The cephalofoil of sphyrnid neonates is curved back along the side of the body thus reducing the amount of frontal area that has to pass through the cloaca of the mother and minimizing the trauma of birth (see Gilbert 1967, Castro 1983). This functional reduction in head width is beneficial whether the shark is born head first or tail first. Immediately post-parturition the head angle decreases (Figure 2.5) which reflects the reorientation of the cephalofoil to a position increasingly perpendicular to the body axis. Among the three species examined, this change in head shape is most conspicuous in the scalloped hammerhead, where the head width is greatest. It is also present to a lesser extent in the bonnethead, although the smaller head width does not necessitate as dramatic a change in morphology.

Electrosensory pore distribution

Despite the fact that the sphyrnids represent the most obvious morphological extreme within the order Carcharhiniformes, the pore distribution patterns on the heads remain recognizable across all three species examined (Figures 2.2, 2.3). In addition to the conservation of pore patterns, the percentage of pores in each of the pore fields is mostly similar across species (Table 2.2). This suggests that the basic pore distribution pattern is conserved across the two genera while still allowing for some flexibility based on the ecology of individual species. Both sphyrnid species examined had a greater

number of pores on the ventral surface of the head whereas the sandbar shark had a more even distribution of pores over dorsal and ventral surfaces of the head. This difference in pore distribution might relate to the feeding ecology of the species. Juvenile scalloped hammerhead sharks feed primarily on benthic prey such as burrowing crustaceans and their associated goby symbiont (Clarke 1971). Bonnethead sharks also feed almost exclusively on benthic crustaceans, such as the blue crab, Callinectes sapidus (Cortes et al. 1996). Juvenile sandbar sharks feed primarily on benthic fishes and crustaceans but also feed to a lesser extent on small fishes in the water column (Medved et al. 1985). Therefore, it would be advantageous for sandbar shark pups to be able to detect potential prey items around the entire head whereas sphyrnids have the highest concentration of electroreceptors on the ventral surface of the head for detection of benthic prey.

Electrosensory pore number

Despite the existence of pore pattern illustrations for several elasmobranch species (Daniels 1967, Gilbert 1967, Raschi 1978, 1984, Chu & Wen 1979), no quantitative comparisons have been performed to determine if sphyrnids have a greater number or density of electrosensory pores compared to carcharhinids. The first prediction of the enhanced electrosensory hypothesis is that sphyrnids should have a greater number of pores compared to carcharhinids which would maintain a comparable pore density over the greater head width. Although the scalloped hammerhead had a greater number of pores than the sandbar shark, the bonnethead had fewer pores. Although the bonnethead had fewer pores than C. plumbeus, it has more than the dusky shark, Carcharhinus obscurus, (mean number of pores = 1896.8, n = 9) (Raschi 1984) and

the gray reef shark, Carcharhinus amblyrhynchos, (number of pores = 1440, n = 1) (Daniels 1967). Thus, the prediction of greater pore numbers in sphyrnid sharks is validated for the scalloped hammerhead but not for the bonnethead shark. To determine whether the number of pores on S. tiburo is atypical of sphyrnid sharks, pore counts must be performed on other sphyrnid species.

Electrosensory pore density

The second prediction of the enhanced electrosensory hypothesis is that the sphyrnids should have a similar, if not greater, density of pores compared to the carcharhinids. A higher pore density implies finer spatial resolution that enables the shark to determine the location of an electrical stimulus near the body surface (Raschi 1978). Although bonnethead sharks could not be tested statistically, there was no significant difference in pore density between the scalloped hammerhead and the sandbar sharks. As the sharks increase in size, the head area and volume increase but the number of pores remains the same. Therefore, the pore density decreases with size (age) of the shark. The decrease in density and attendant resolution might not be a detriment to larger scalloped hammerhead sharks because they inhabit clear oceanic water where vision can play a more important role in prey detection (Compagno 1984). As juveniles, scalloped hammerhead pups inhabit turbid bays where vision is limited and where they might need to rely on other senses for prey detection (Clarke 1971, Compagno 1984). Therefore, it is advantageous for the pups to have the highest density of pores when they are most needed.

Although S. lewini had a greater head width (Figure 2.4) and surface area (Figure 2.6), it did not significantly differ in head volume compared to C. plumbeus. This is ascribed to the large, flat, wing-like cephalofoil of S. lewini that serves to maximize area with minimal volume. The comparable pore densities between S. lewini and C. plumbeus are attributable to the greater number of pores over the greater surface area of the head in S. lewini. This results in no net loss of resolution compared to similar sized C. plumbeus. The decrease in pore density and resolution with increasing size (age) of the sharks might be compensated for by an increase in sensitivity. Sensitivity to electric stimuli is a function of the population of receptor cells within the ampulla proper (Raschi 1986) and length of the ampullary canal (Murray 1974). A larger ampulla will provide for a greater population of receptor cells which will enhance sensitivity and signal-to-noise ratio (Raschi 1986). Also, long canals are more sensitive to weak electric stimuli than are short canals (Obara & Bennett 1972; Bennett & Clusin 1978). Therefore, along with the increase in shark size, the size of the ampullae and length of the ampullary canals will increase thus increasing the sensitivity of the electroreceptors. The decrease in resolution might be offset by an increase in sensitivity resulting from canal elongation, thus resulting in no overall change in electroreceptive capacity.

This study provides evidence that the head morphology of sphyrnid sharks is concordant with the assumption and predictions of the enhanced electrosensory hypothesis. The greater number of receptors with an equivalent packing density distributed over a laterally expanded head morphology indicates that the sphyrnid cephalofoil demonstrates the characteristics expected of a head that is optimized for electroreception. Although the sphyrnid head morphology supports the predictions of the

enhanced electrosensory hypothesis, behavioral tests are needed to examine whether sphyrnids are able to utilize their unique cephalofoil to detect and resolve electric stimuli to a greater extent than similar sized carcharhinids.

Table 2.2 Head morphology measurements expressed as percentage of total length for three shark species. The morphometrics include head width (HW), head length (HL), trunk width (TW), mouth width (MW), mouth to snout distance (MS) and internarial distance (IN).

	S. lewini				S. tiburo				C. plumbeus			
	Mean	SD	Range	n	Mean	SD	Range	n	Mean	SD	Range	n
HW	27.4	2.5	21.5-32.6	51	17.7	1.9	15.0-20.6	48	11.7	0.9	9.8-12.9	23
HL	12.8	1.4	8.6-14.8	50	15.3	2.2	12.0-18.3	47	16.0	1.0	13.5-17.3	23
TW	9.1	0.5	7.8-10.2	50	10.6	0.9	9.1-12.4	47	12.9	0.7	11.6-14.0	23
MW	6.2	0.4	5.4-7.0	51	6.9	0.6	6.1-8.6	46	8.7	0.6	7.0-9.7	23
ML	3.3	0.3	2.6-4.0	51	3.8	0.3	3.0-4.3	46	4.5	0.2	4.1-4.9	23
MS	6.6	0.9	4.3-7.7	50	7.9	1.3	6.0-9.7	47	7.8	0.7	6.3-8.8	23
IN	18.9	1.4	16.5-22.0	51	11.8	1.4	9.8-14.0	47	6.1	0.3	5.5-6.6	23

Table 2.3 Percentage of mean number of pores in each dorsal and ventral pore field (Figures 2.2, 2.3) for the scalloped hammerhead, bonnethead and sandbar sharks. The percentage of pores in each pore field is comparable across species even though the total number of pores differs.

Species	Dorsal pore fields				Ventral pore fields							
	a	b	c	d	e	f	g	h	i	j	k	l
S. lewini	12.4	10.2	3.4	15.0	11.1	3.6	11.4	8.7	2.3	19.6	1.7	0.7
S. tiburo	11.8	14.5	4.0	15.1	9.7	3.7	12.1	6.4	3.0	16.2	1.8	1.7
C. plumbeus	12.3	18.8	2.8	16.5	6.8	5.3	14.5	5.0	4.2	10.5	1.8	1.4

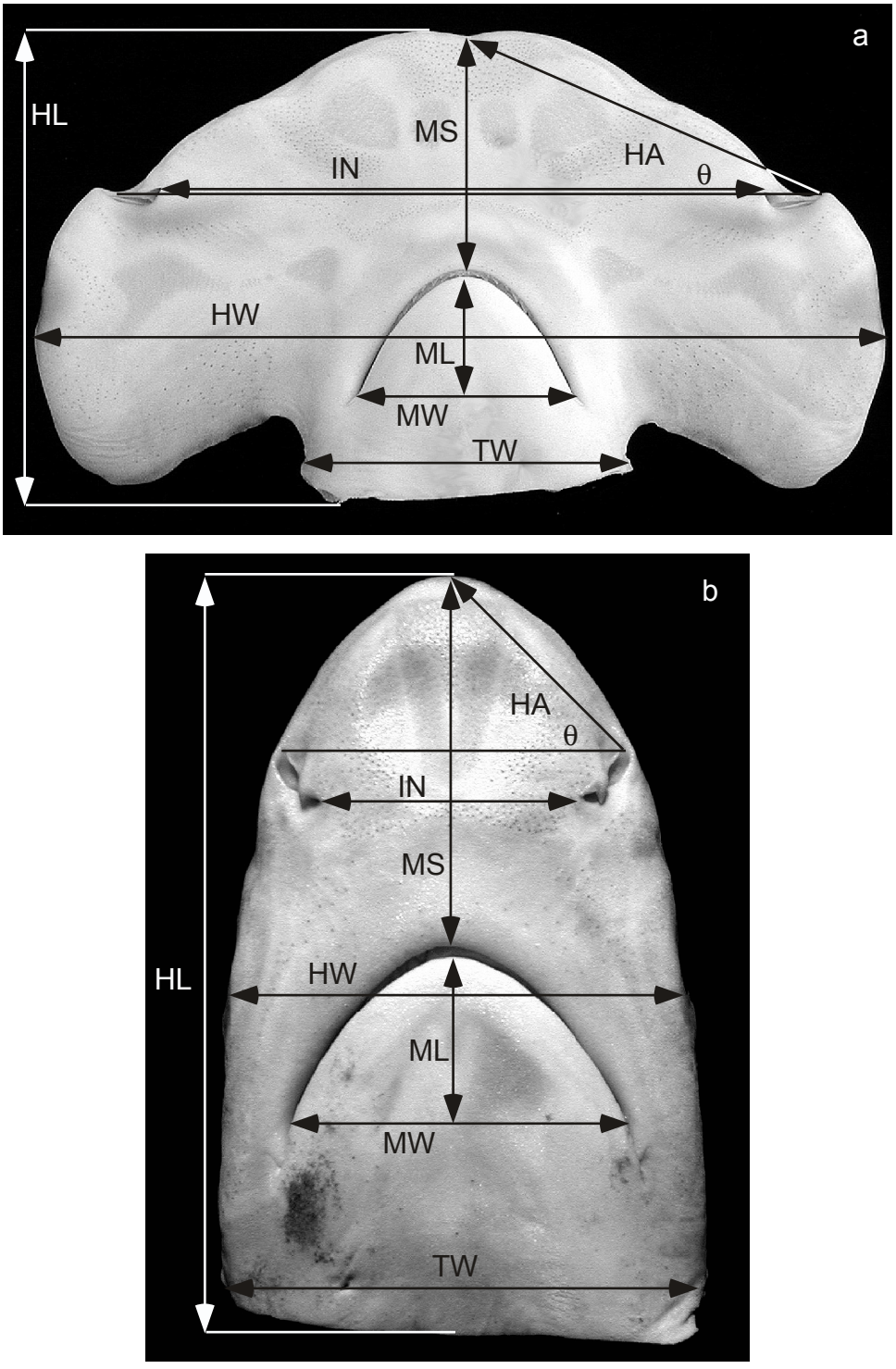

Figure 2.1. Photograph of the head of (a) a scalloped hammerhead shark and (b) a sand-bar shark indicating head morphometrics measured on each individual. Morphometrics included head width (HW), head length (HL), trunk width (TW), mouth width (MW), mouth length (ML), mouth to snout distance (MS), internarial distance (IN) and head angle (HA). Volume and surface area of each head were also measured.

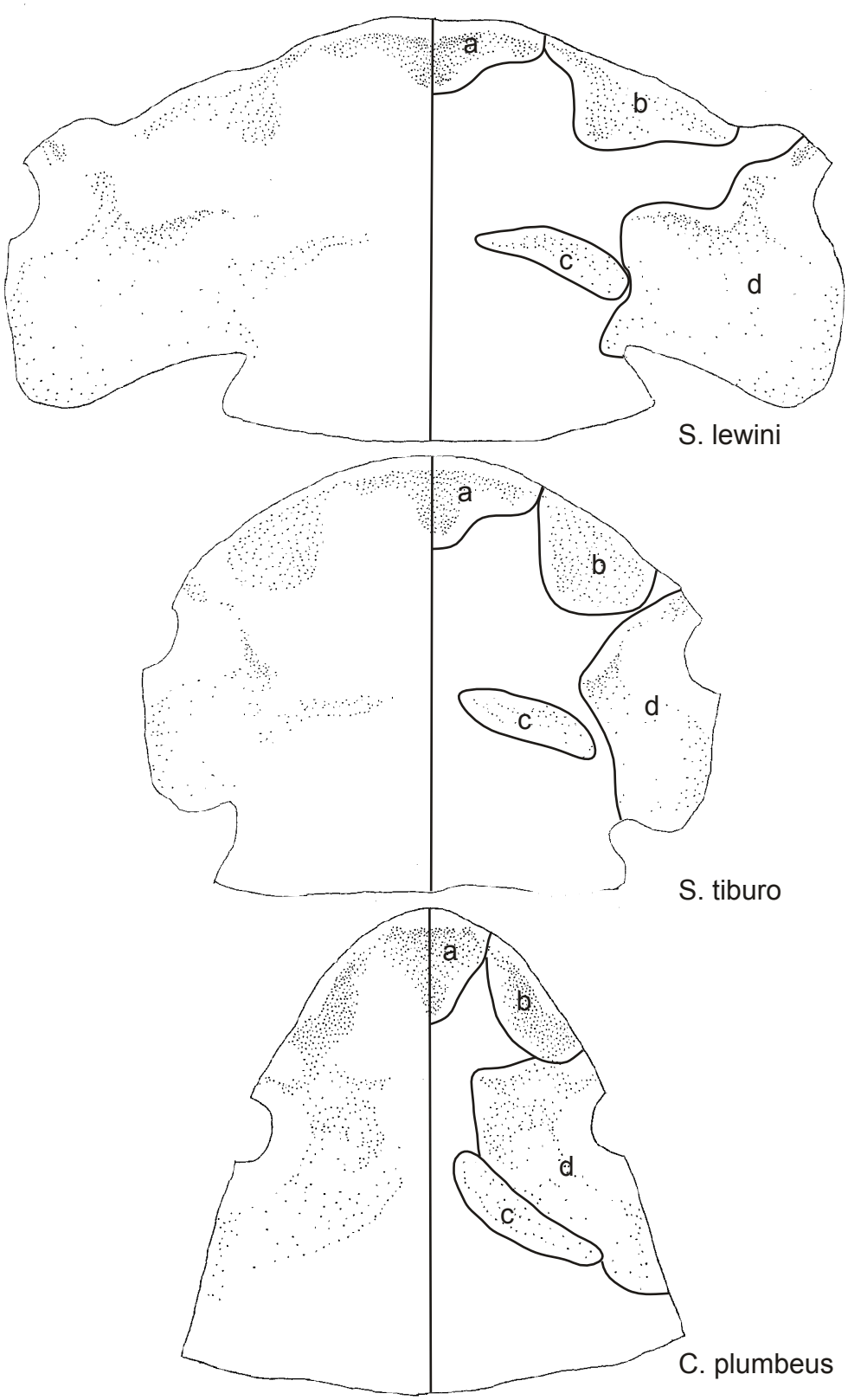

Figure 2.2 Distribution pattern of electroreceptor pores on the dorsal surface of the head of scalloped hammerhead, bonnethead and sandbar sharks. Pore are illustrated on the entire dorsal surface and the right side of each head is subdivided into four pore fields (a-d) which correspond across species.

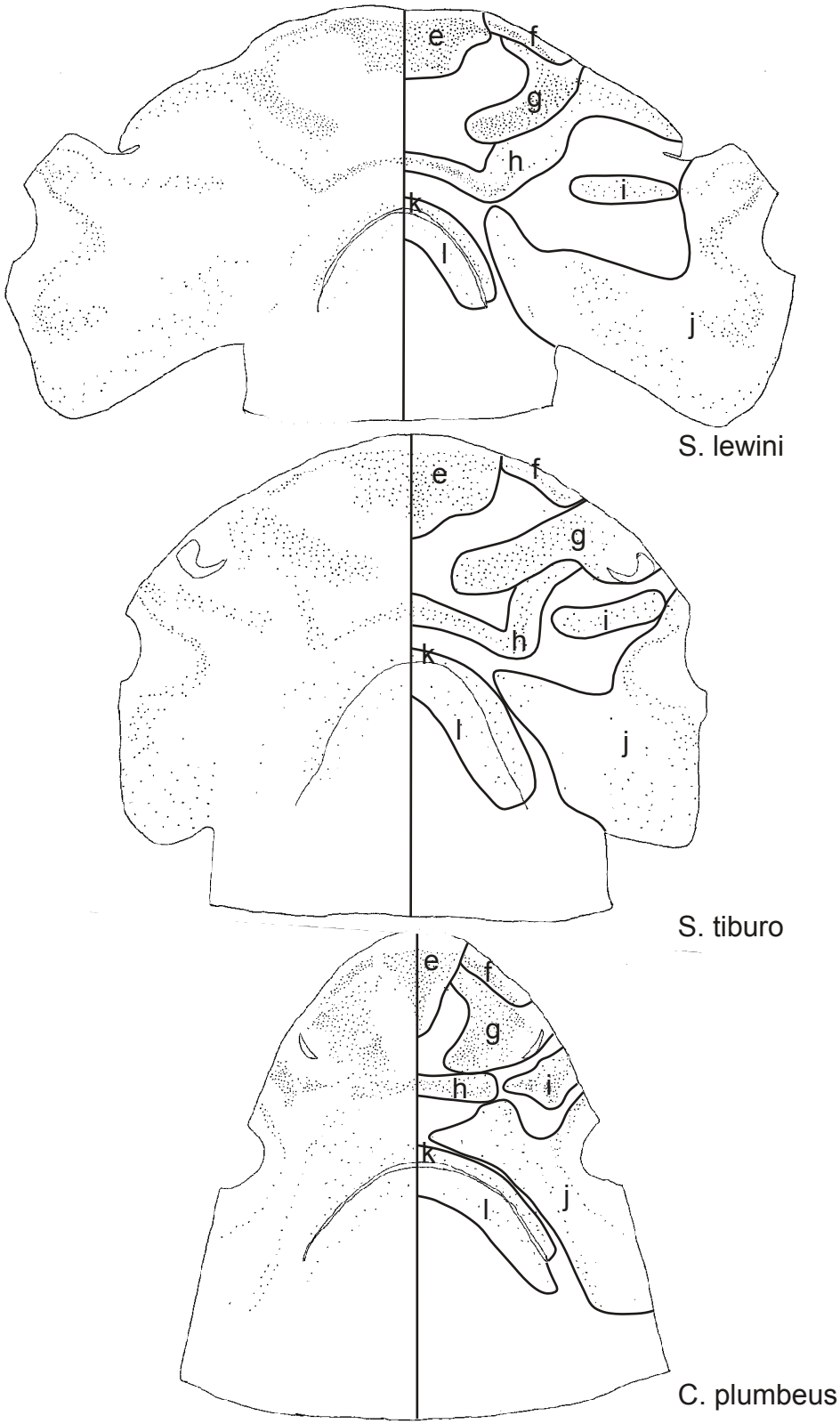

Figure 2.3 Distribution pattern of electroreceptor pores on the ventral surface of the head of scalloped hammerhead, bonnethead and sandbar sharks. Pore are illustrated on the entire ventral surface and the right side of each head is subdivided into eight pore fields (e-l) which correspond across species.

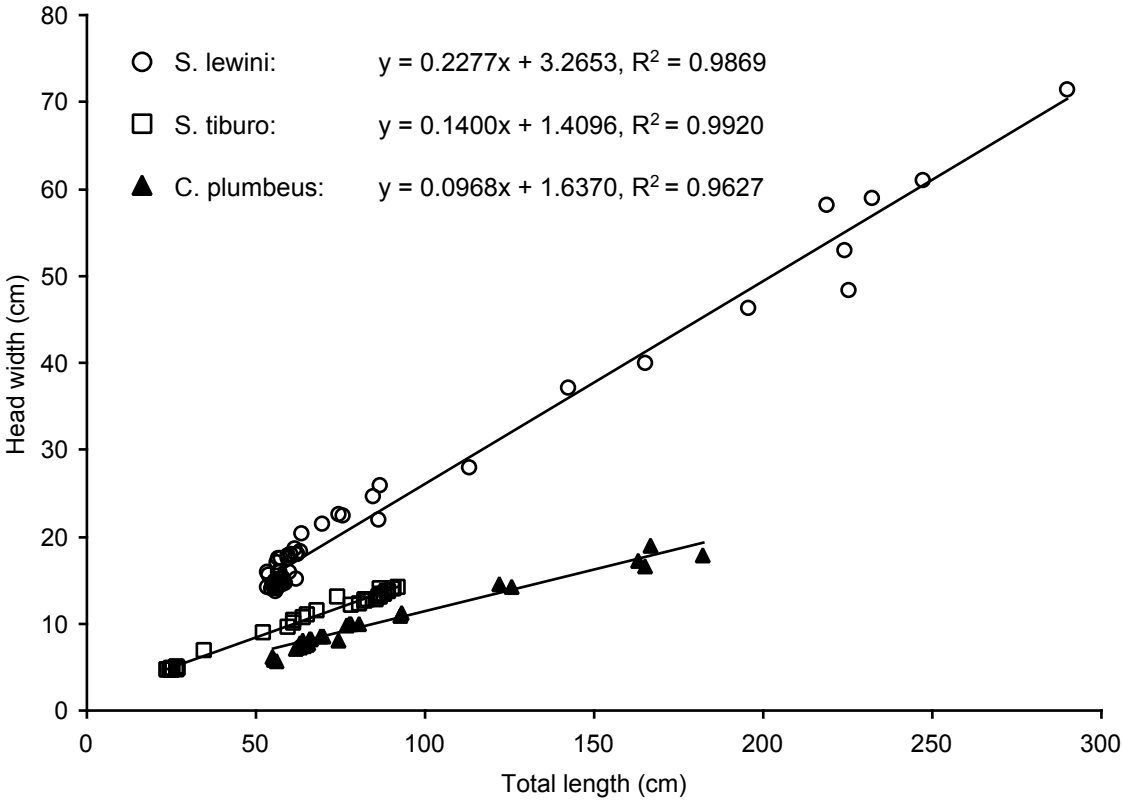

Figure 2.4 Head width as a function of shark total length for scalloped hammerhead, bonnethead and sandbar sharks. Whereas head width increases linearly with shark size for the bonnethead and sandbar sharks, there is a dramatic increase in head width seen in immediately post-parturition scalloped hammerhead shark pups.

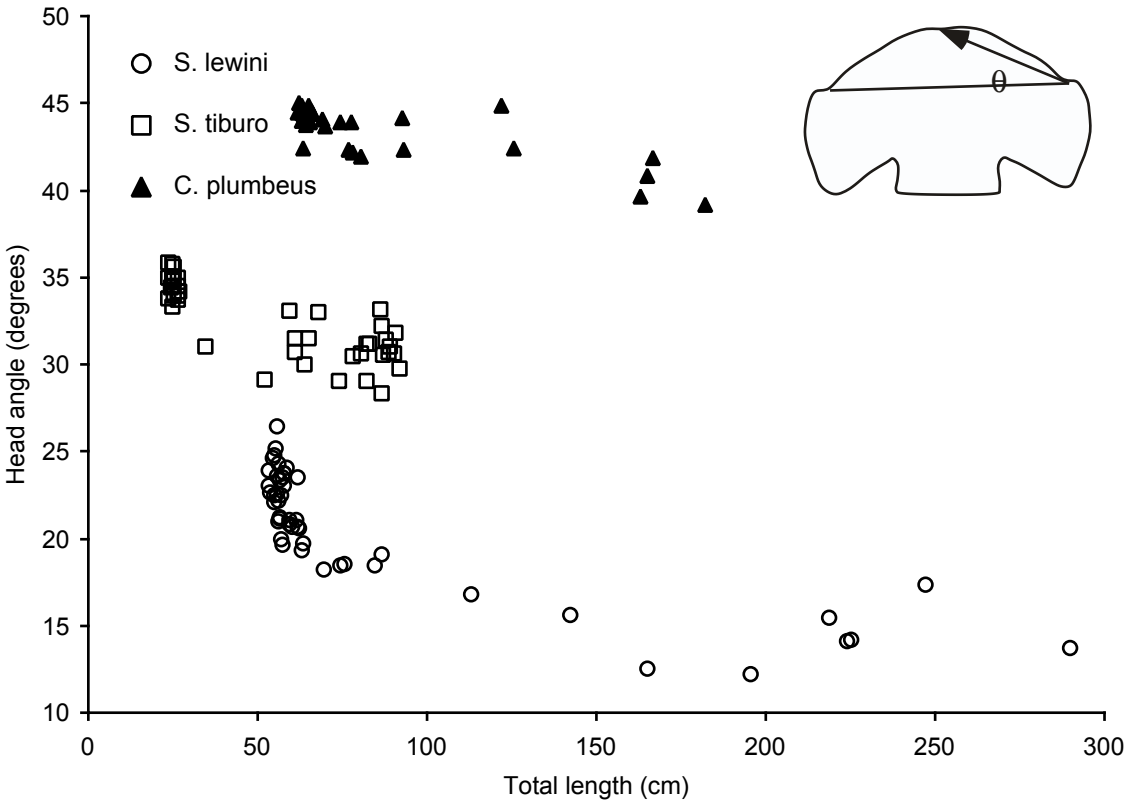

Figure 2.5 Anterior head angle as a function of total length for three shark species. Head angle decreases linearly in neonates to adults for sandbar sharks whereas a dramatic decrease in head angle is seen in post-parturition scalloped hammerhead shark pups. A smaller decrease in head angle is seen in bonnethead shark neonates.

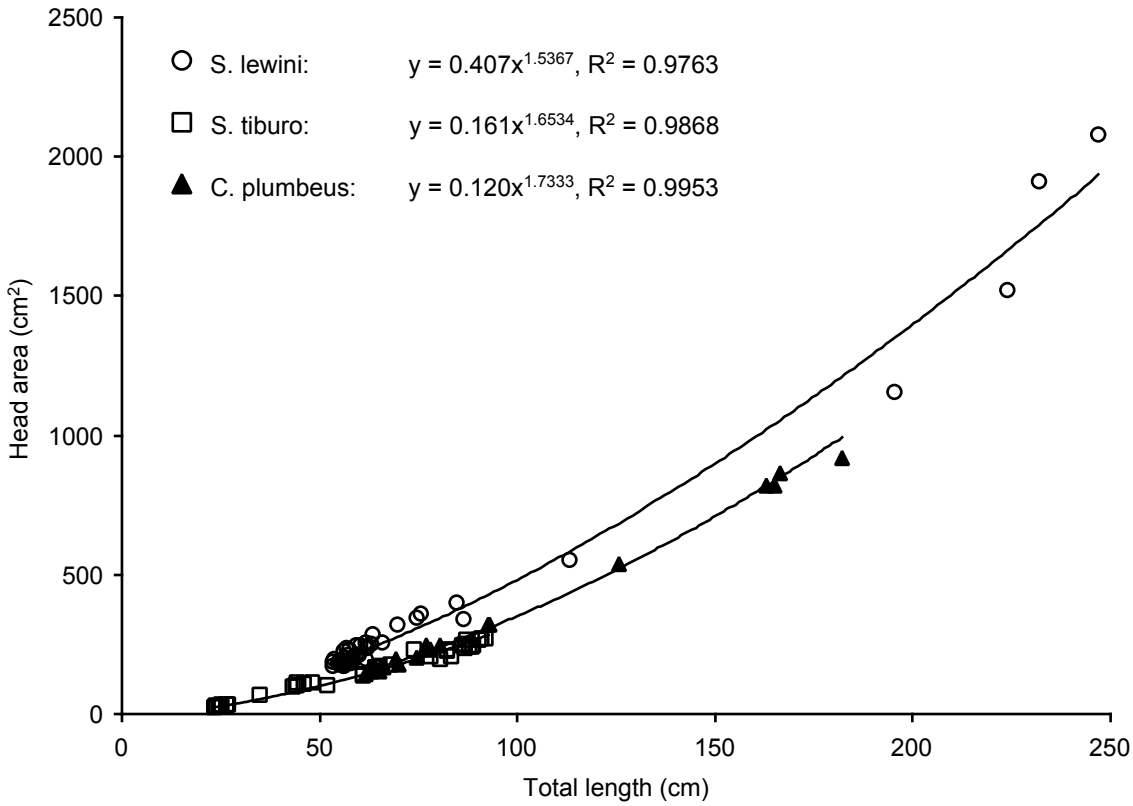

Figure 2.6 Surface area of the head of three shark species. For any given size, the scalloped hammerhead has a greater head area than the sandbar shark. The bonnethead shark could not be statistically analyzed.

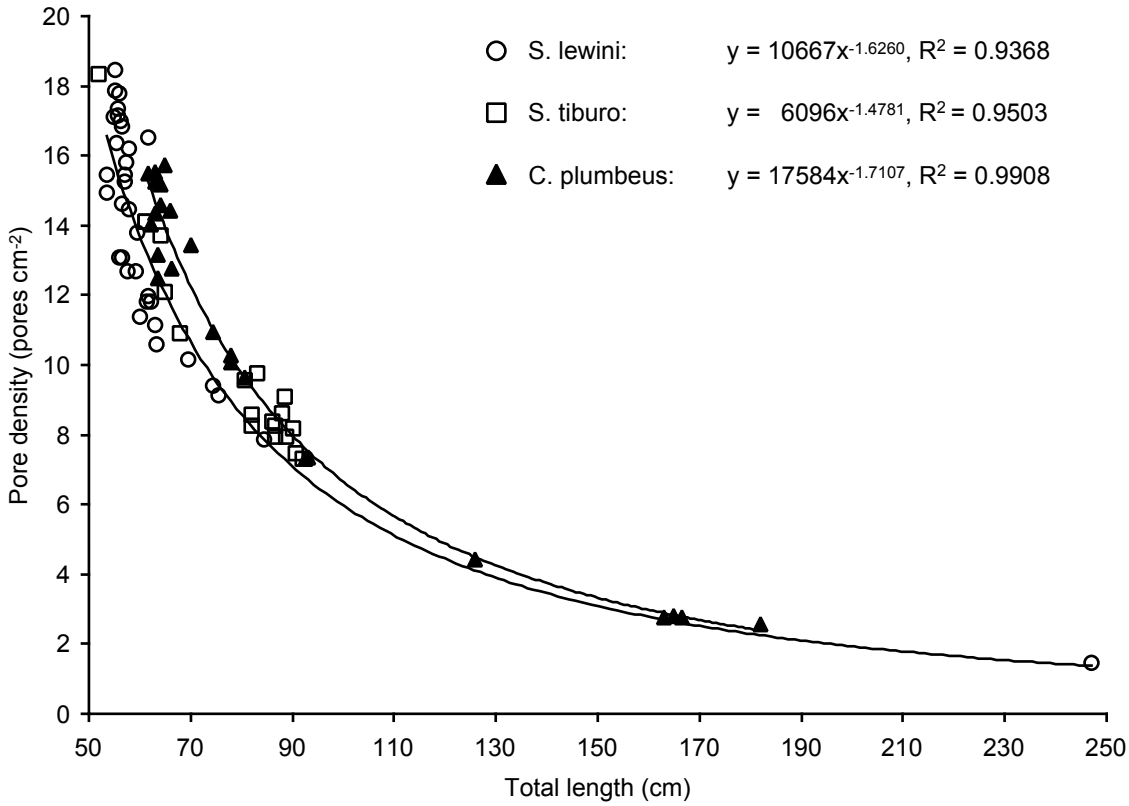

Figure 2.7 Electrosensory pore density (pores cm^{-2}) of scalloped hammerhead, bonnethead and sandbar sharks. Juvenile scalloped hammerheads have the greatest maximum pore density and density is inversely proportional to the size of the shark. There is no significant difference in pore density between scalloped hammerhead and sandbar sharks.

CHAPTER 3

RESPONSE OF JUVENILE SCALLOPED HAMMERHEAD SHARKS, SPHYRNA LEWINI, TO VARIOUS ELECTRIC STIMULI

INTRODUCTION

The ability of elasmobranchs to orient to electric fields is well documented. However, although several species have been studied for electroreceptive response (Chapter 1), no studies have investigated the electrosensory capabilities of sphyrnid sharks. This absence of experimental investigation into sphyrnid electroreception is surprising given that it has been hypothesized that the sphyrnid head morphology might have evolved to increase sampling area and sensitivity to electric fields (Compagno 1984; Kajiura 2001). This study quantified the responses of juvenile scalloped hammerhead sharks, Sphyrna lewini, to prey-simulating dipole electric fields and compared the hammerhead shark sensitivity to the sensitivity of other species described in the literature.

The response of the sharks was tested by using a dipole electric field to approximate the standing d.c. field that surrounds living organisms in seawater (Kalmijn 1972, 1988). By manipulating parameters such as the separation distance of the poles on the dipole and the magnitude of the electric current passed between the electrodes, various electric field sizes and intensities were generated. These various field characteristics were used to test predictions about the response of the sharks to electric stimuli. It was predicted that the sharks would orient from a greater distance when exposed to larger dipole separations because a larger dipole separation will create a

proportionally larger electric field when current is held constant. Similarly, sharks should also orient from a greater distance when exposed to a dipole with a greater applied current strength when dipole separation distance is constant. Implicit in these predictions is the assumption that the dipole parameters remain sufficiently naturalistic that the sharks will demonstrate a natural feeding response. It was further predicted that the sharks would demonstrate the best response (lowest stimulus threshold) to stimuli that most closely resemble their natural prey. These predictions were tested by quantification of the response distance of the sharks to various stimuli and subsequent calculation of the minimum voltage gradient that elicited a response (i.e., their threshold sensitivity).

Studies of electroreceptive response typically use a dipole to simulate the electric field of a prey item (Kalmijn 1971, 1982; Johnson et al. 1984; Tricas 1982). Although various investigators have mathematically modeled an ideal dipole electric field in seawater (Kalmijn 1982; Johnson et al. 1984; Tricas et al. 1995), there are no published accounts of a dipole electric field in seawater being empirically measured to verify the theoretical charge distribution. Thus, this study also measured the electric field in seawater and compared it to the calculated theoretical distribution of electric charge for an ideal dipole.

METHODS

Facilities

Juvenile scalloped hammerhead sharks, S. lewini, were caught in Kaneohe Bay, Oahu, by hand line fishing with barbless hooks, which minimized damage to the mouth

area. Immediately after being brought to the surface, the sharks were dehooked, placed in a 1m diameter, seawater-filled, fiberglass hemisphere and quickly transported to the outdoor shark pens at the Hawaii Institute of Marine Biology (HIMB), Coconut Island. The sharks were fed to satiation on a diet of cut squid and fish every other day and were allowed to acclimate to the pen for a minimum of one week prior to testing.

The pen in which experiments were conducted was approximately 10.2 x 19.4m with a maximum depth of 2.4m. The pen was bounded by fences at both ends that enclosed the sharks but allowed tidal flushing of water and small reef fish to move through freely into the pen. Because the pen was merely an enclosure of part of the natural reef, the habitat in the shark pen was representative of the reef habitat in Kaneohe Bay and included live coral, various reef fishes and invertebrates. Thus, the pen represented a semi-natural habitat complete with typical reef fauna.

The shallow (< 0.5m) part of the experimental pen was used as the test arena. This area was chosen because at low tide the shallow depth facilitated videotaping of the sharks with an overhead camera. A barrier net was deployed across the width of the pen to isolate the shark being tested from others in the deeper part of the pen. Individually testing each shark eliminated interaction effects from other individuals that might also attempt to bite at the electrodes.

Experimental apparatus

A stimulus generator was designed to apply prey-simulating dipole electric fields to the seawater (Figure 3.1). The stimulus generator was comprised of a battery-powered circuit that passed electric current through the seawater, which acted as a resistor in the

circuit. The circuit consisted of an on/off switch, a low/high power switch that engaged or disengaged a 1MΩ resistor, an external power source switch that enabled the operator to switch from the internal 9V battery to an external power source, a four-position rotary switch that switched between the four dipole pairs and a 1MΩ potentiometer that was used to adjust current flow through the circuit. The stimulator enabled the experimenter to vary the strength of the applied stimulus current and to switch between any of the four dipole pairs. An ammeter in series allowed the experimenter to monitor the amount of current being applied through the circuit.

Current from the stimulus generator was delivered to the target dipoles via underwater cables and seawater-filled tygon tube salt bridges. Four pairs of shielded 18AWG SO underwater cables were plugged into the stimulus generator. The cables passed current to seawater-filled tygon tubes via underwater connectors with gold-plated stainless steel pins. One end of a 50cm length of tygon tubing was fitted snugly over the rubber sleeves that partially encased the pins of the underwater connectors. The seawater-filled tygon tubing formed a salt bridge between the underwater connector and the electrode array. The electrode array consisted of a $1m^2$ clear acrylic plate that was divided from the corners into four quadrants of equal area (Figure 3.2). Within each quadrant, a pair of holes was drilled with separations of 1, 3 or 5cm. These dimensions reflected the size of naturally occurring prey items in the stomach of juvenile hammerhead sharks (Bush, pers. comm.). The salt bridges were inserted through the holes from the bottom of the plate and were flush with the upper surface. In the center of the plate and equidistant (25cm) from the center of each electrode pair was a single hole

that was used to introduce an odor stimulus to the testing arena. An odor delivery tube was flush-mounted to the surface of the plate from the bottom and extended from the hole in the center of the plate to a syringe on the surface. The syringe was fitted with a 3-way valve that allowed the experimenter to draw an odor stimulus (squid rinse) from a bucket on the surface and remotely introduce the odor to the center of the electrode array. Although the clear acrylic plate could be seen by the sharks, its primary function was to mask extraneous electric fields in the immediate vicinity of the dipoles. Therefore, any bite responses were attributable to the electrodes and not natural prey items nearby.

A Hi8 video camera mounted on a moveable track approximately two meters above the surface of the water was positioned directly over the plate (Figure 3.3). The camera record and stop functions were also operated by remote control, which minimized extraneous experimenter movements during an experimental trial. Experiments were conducted primarily at low tide to minimize water distortion of the video image, and the camera was fitted with a polarizing filter that reduced surface glare.

Experimental protocol

At the beginning of each trial, a single shark was introduced to the testing arena and allowed to acclimate for several minutes. A well-acclimated shark would swim throughout the entire pen and not limit itself to swimming along the edge of the pen or along the barrier net. To stimulate the shark to start to search for food, an olfactory cue (squid rinse) was introduced to the pen via the odor delivery tube. During each trial, only one of the four dipoles on the acrylic plate was active at any given time while the other three served as controls. When the shark detected the odor and began to demonstrate

searching behavior (as indicated by increased tail beat frequency, frequency of turning and swimming close to the bottom) the video camera was activated and the shark's response to the electric field was recorded on Hi8 videotape at 30 frames per second (fps). A continuous audio commentary of the shark's movements and behavior was recorded on the audio track of the videotape. After the shark bit at a dipole, that dipole was turned off and another dipole was activated. Trials were brief because the shark would become unresponsive (as indicated by decreased tail beat frequency, frequency of turning and swimming throughout the water column) after a couple of minutes. At the end of each trial the shark was fed to satiation and allowed to rejoin the others on the opposite side of the barrier net. Any excess food was removed from the pen prior to introduction of the next individual to the testing arena. The protocol was repeated for up to eight individuals per day. At the end of an experimental session, all sharks were fed to satiation and then starved for two days prior to the next set of trials. Because the sessions were always conducted after two days without food, hunger, and hence motivational state, was controlled and considered comparable among trials.

Two variables were manipulated in the experiments. In one set of experiments, a constant current was applied across dipole separations of various sizes (1, 3, 5cm). The other manipulation varied the amount of electric current (5.0 to 8.9μA) across a constant dipole separation distance. The range of currents was at the low extreme of potentials measured from prey (Kalmijn 1972) and was chosen based on literature values which had successfully elicited feeding behavior in other elasmobranch species (Kalmijn 1971, 1978, 1982). The manipulation of dipole separation distance and applied current strength produced a range of d.c. dipole moments. For example, 5μA of electric current applied

across a 1cm dipole separation distance results in a dipole moment of 5μA cm, whereas a current of 8μA applied across a 5cm dipole separation distance results in a dipole moment of 40μA cm.

Analysis

The Hi8 video footage was digitized on a computer equipped with a video digitization board that captured a high resolution image (640 x 480 pixels) of each frame at 30fps. Digital movies of 320 x 240 pixels, 30fps were constructed of each bite at the dipole. The reduced size was necessary to allow the video to play from a cd-rom at full motion 30fps. Each sequence would start with the frame in which the shark entered the field of view and would end when the shark bit the dipole and swam out of the field of view. The criteria used to define biting behavior were deliberately conservative and bites were considered to have occurred only if the shark clearly snapped its lower jaw in an attempt to bite at the electrodes. Biting behavior could be reliably detected on the video record by observing the shark positioning its head directly over the electrodes and the gill flaps flaring as water was passed through the mouth and over the gills.

Frame-by-frame analysis of the video footage enabled the quantification of orientation distance to the dipole and the position of the shark relative to the dipole axis (Figure 3.4). An orientation toward a dipole was defined as a deviation of greater than 20° from the preceding course trajectory. The resulting change in trajectory would result in any portion of the shark's head passing directly over the active dipole. The frame in which the shark initiated its orientation to the dipole was captured and copied to an image

analysis program (NIH Image v1.6.1). The 20cm diameter frame-of-reference circle drawn around each dipole was used to calibrate the image analysis software. The orientation distance was measured from the center of the dipole to the closest side of the shark's head. This provided a more conservative estimate of orientation distance than measuring to the center of the head which would add several cm to the maximum orientation distance. The orientation distance data were tested for normality and homoscedasticity prior to analysis with a 2-way ANOVA using dipole separation and applied current strength as the two treatments. In addition to the orientation distance, the initial angle of the shark with respect to the dipole axis was also measured (Figure 3.4). From these data (distance and angle with respect to the dipole axis) the electric field intensity (= voltage gradient, V cm^{-1}) at the position where the shark initiated a turn toward the electrodes was calculated using the ideal dipole field equation from Kalmijn (1982). This electric field intensity value was taken as the behavioral response threshold of the sharks to the electric stimulus. This technique has been used by previous investigators to estimate the minimum electric field intensity that elicits a response by elasmobranchs (Kalmijn 1971, 1978, 1982; Johnson et al. 1984).

Electric field measurement

To verify that the calculated electric field intensity values (based on distance and angle of the shark with respect to the center of the dipole) matched actual values experienced by the sharks, a dipole electric field was measured in a controlled environment. The experimental apparatus used is illustrated in Figure 3.5.

An acrylic tank (63 x 93 x 32cm) was filled to a depth of 23cm with seawater from Kaneohe Bay. Two holes separated by 1 cm were drilled through the center of a 71.5 x 59cm acrylic plate. The acrylic plate was marked with concentric circles of 5, 10, 15 and 20cm radius around the center of the 1cm dipole. Radiating from the center of the dipole were lines drawn at 0°, 30°, 60° and 90° with respect to the dipole axis. Fifty cm lengths of seawater-filled tygon tubing were pressed through the bottom of the acrylic plate so the tips of the tubing were flush with the surface of the plate. The plate was then placed on the bottom of the tank. The opposite end of each length of tubing was tightly sealed to gold-plated stainless steel pins at the end of underwater cables. The underwater cables were the same as those used in the field experiments. A function generator was used to apply a 0.1kHz sine wave signal across the electrodes.

The voltage at various locations in the tank was measured with silver/silver chloride electrodes connected to an amplifier and oscilloscope. The reference electrode was affixed to the side of the tank near the surface of the water as far as possible from the center of the dipole. The recording electrode was offset 1cm from the end of a glass rod and was moved to various points around the acrylic plate to sample the voltage. Voltage was measured by observing the magnitude of the sine wave trace on the oscilloscope. Prior to taking each measurement, the recording electrode was placed next to the reference electrode and the oscilloscope was zeroed. Measurements were made of the field at 5, 10, 15 and 20cm radius and at angles of 0°, 30°, 60° and 90° with respect to the dipole axis. Values obtained at each position were transformed to a relative scale to range from a maximum of 1.0 at 5cm, 0°, and compared to values calculated for an ideal

dipole charge distribution. Electric field intensity (voltage gradient) was derived directly from the measured voltages at known distances from the center of the dipole.

RESULTS

Electric field measurement

The measured voltages closely matched the values calculated for an ideal dipole distribution. The voltage decreased as a cube of distance, and the standard deviation error bars enclosed the ideal (calculated) values (Figure 3.6a). The voltage also varied as a cosine function of angle around the dipole axis. The voltage was greatest in the plane of the dipole axis (0°) and decreased to zero in the perpendicular plane (90°). Again, the standard deviation error bars of the measured values enclosed the ideal values (Figure 3.6b). The close match between measured and calculated voltages indicates that the electric field intensity can be accurately interpolated for any position around the dipole.

Behavioral response

Feeding responses (bites) were obtained for all dipole sizes and applied current strengths. Sharks oriented to the center of the dipole by turning sharply (> 20° change in trajectory), swimming directly toward the center of the dipole and biting at the electrodes. This behavior was initiated from a maximum distance of 36.3cm. Sharks that were stimulated to search for food always bit at the active dipole when they passed within the 10cm radius frame-of-reference circle drawn around each electrode pair. Sharks never bit at the non-active (control) dipoles. Multiple bites at the active dipole were sometimes observed. Sharks would bite once then immediately swim away, turn back and bite at the

dipole again, often repeatedly. In these instances, only the initial orientation was included in analyses as subsequent orientations might have derived from the shark knowing the location of the dipole from the initial interaction.

Orientation distance

Because size of the electric field increases proportionally with dipole separation distance when current is held constant, it was predicted that the sharks would orient from farther away as the dipole separation increased from 1 to 5cm. Consequently, response distances were compared for the three dipole separation distances (1, 3, 5cm). The sharks demonstrated a significant difference in orientation distance with increased dipole separation at constant current (Figure 3.7, 2-way ANOVA, $F_{3,253} = 2.633$, $p = 0.0498$). Sharks oriented to the 5cm dipole from a greater distance than they did from the 1 cm dipole (Fisher's PLSD, $p = 0.0322$). The mean orientation distance for the 1cm dipole was 10.9±0.50SE cm and for the 5cm dipole was 12.9±0.86SE cm. The mean orientation distance for the 3cm dipole was intermediate at 12.1±0.51SE cm and the orientation distance to the 3cm dipole did not differ from either the 1cm or 5cm dipoles (Fisher's PLSD, $p = 0.1200$ and $p = 0.3549$ respectively).

Although the sharks followed the predicted pattern and oriented from a greater distance at greater dipole separations, they did not orient from a greater distance at greater applied current strengths for any given dipole separation distance (Figure 3.8, 2-way ANOVA, $F_{2,353} = 2.722$, $p = 0.0671$).

Threshold sensitivity

The minimum electric field intensity that elicited a response is a measure of the threshold sensitivity of the sharks. Approximately 4.7% of all responses were elicited at electric field intensities of less than 2 nV cm^{-1}, 1.9% of responses were elicited at electric field intensities of less than 1 nV cm^{-1} and 0.8% of responses were to electric field intensities of less than 0.5 nV cm^{-1}. The median electric field intensity that resulted in the initiation of a response to a 1cm dipole was 24.9 nV cm^{-1}. For the 3cm dipole the median electric field intensity was 69.5 nV cm^{-1} and for the 5cm dipole the median electric field intensity was 82.6 nV cm^{-1}. Therefore, the sharks demonstrated the greatest sensitivity (i.e., responded at the lowest electric field intensity) when exposed to the smallest (1cm) dipole. This indicates that the sharks demonstrate the greatest sensitivity to small dipole separations that probably represent the size of their most common prey.

DISCUSSION

This study is the first to examine electroreception in a sphyrnid shark and to quantify the response of any elasmobranch to a variety of prey-simulating electric fields to test predictions about their behavioral response. Requisite to the data collection of shark responses to electric fields in seawater was verification that the equation used to calculate electric field intensity (voltage gradient) accurately represented the actual field intensity. Therefore, this study also measured the electric field intensity of a test-type dipole in seawater and compared the measured values to values modeled by the ideal dipole field equation.

Electric field measurement

A dipole electric field in seawater is modeled by the equation: $E = \cos\theta\left(\frac{\rho I d}{\pi r^3}\right)$ (Kalmijn 1982). The variables include: ρ = resistivity of the seawater (Ωcm), I = applied electric current (A), d = dipole separation distance (i.e., distance between positive and negative poles of the dipole) (cm), r = radius distance (i.e., distance from the center of the dipole to the position of the shark's head at the point where the shark initiates its orientation to the dipole) (cm) and θ = angle with respect to the dipole axis (Figure 3.4). This equation describes an electric field in half space, with the electrodes mounted to the base of an insulating plate such that the conducting medium is a hemisphere above the electrodes (Kalmijn 1982). From this equation it is apparent that the ideal dipole decreases in electric field intensity (E) as an inverse cube of distance (r). The field intensity of an ideal dipole also varies as a function of angle with respect to the dipole axis. The field intensity is maximal in the plane of the dipole axis (0°) and decreases as a cosine function to a theoretical null in the perpendicular plane (90°). The empirically measured values closely matched the calculated ideal values for both components (Figure 3.6). For each experimental trial, the appropriate values of distance (r) and angle (θ) were used to determine the electric field intensity at the point where the shark initiated its orientation to the dipole (Figure 3.4). The close concordance between the measured and calculated values confirms that the response thresholds calculated for the sharks based on distance (r) and angle (θ) accurately represent the actual field intensities encountered by the sharks.

The equation used to model the electric field intensity assumes that the orientation distance exceeds that of the dipole separation distance (r>>d) (Kalmijn 1982). This equation has been used in other studies of elasmobranch electroreception (Kalmijn 1982, Johnson et al. 1984) and is sufficient for the resolution obtained in this study. That is, since the head of the shark is large with respect to the dipole separation distance, there is no single point along the head that can be taken as the detection point. This study chose the point along the side of the head that was closest to the center of the dipole. Therefore, the calculated field intensity should be used as an approximation and not a definitive measure of threshold sensitivity. The value of this technique is in its comparison of relative field intensities rather than determination of absolute sensory capabilities. The measurements were taken from the center of the dipole to the edge of the head closest to the dipole rather than to the center of the head (Figure 3.4). This is particularly important for sphyrnid sharks in which the distance from the edge of the head to the center can be large. Therefore, measurement to the center of the head could increase the orientation distance by several cm. By measuring from the center of the dipole to the edge of the head, more conservative estimates of the shark's sensory abilities were derived.

Behavioral response

The fact that the sharks bit at the dipoles attests to the adequacy of the stimulus to represent prey. The sharks initiated orientations from distances in excess of 30cm and demonstrated their ability to precisely locate the dipole source by biting only when directly over the center of the dipole. The non-active (control) dipoles were never bitten even though they were visually identical to the active dipole.

Orientation distance

Two parameters, dipole separation distance and applied current strength, were manipulated to test for differences in orientation distance to different stimulus conditions. The 1cm, 3cm and 5cm dipoles simulated small, medium and large prey items for this size of shark and the electric current strengths, from 5.0 to 8.9μA, were used to generate prey-simulating electric fields. A given electric field intensity will occur at a greater distance from the center of the dipole when the separation distance between the poles is increased creating a greater d.c. dipole moment (Figure 3.9a). Therefore, it was predicted that for a given electric field intensity (E) the sharks would orient to a dipole from a greater distance (r) when the separation between the poles (d) was increased: $\left(E \propto \frac{d}{r^3} \right)$. That is, the sharks will encounter a given electric field intensity at a greater distance from the center of the dipole when the dipole separation distance is increased (Figure 3.9a). For example, a shark capable of detecting an electric field intensity of 0.01μV cm^{-1} would encounter that value at 15.1cm from the center of the dipole if the poles were separated by 1cm (6.0μA x 1cm = 6μA cm dipole moment). That same electric field intensity would occur at 25.8cm from the center of the dipole if the poles were separated by 5cm (6.0μA x 5cm = 30μA cm dipole moment). (This example assumes average testing conditions with an applied current of 6.0μA, a seawater resistivity of 18Ωcm and an orientation angle of 0°) Therefore, increasing the dipole separation from 1cm to 5cm would provide a greater than 70% increase in possible detection distance for this example. The prediction of increased orientation distance with increased dipole size was

supported by the data. The sharks oriented from a significantly greater distance when exposed to a 5cm dipole compared to a 1cm dipole (Figure 3.7).

Although the sharks oriented from a significantly greater distance when the dipole separation distance was increased, if the dipole separation distance exceeds the size of a natural prey item the sharks might not interpret the larger electric field as prey. Therefore, the behavior of the sharks may be influenced by their perception of the stimulus and they might not respond as predicted, if the parameters are extrapolated beyond certain limits. For instance, if the dipole separation is exceedingly large, the sharks might not bite at the dipole but might actually be repelled. Because this study examined only prey-simulating stimuli, this hypothesis remains to be tested.

A given electric field intensity will also occur at a greater distance from the center of the dipole when the applied current strength is increased (Figure 3.9b). Therefore, if sharks respond by orienting to the dipole when they detect some threshold electric field intensity (E), it was predicted that the sharks would orient from a greater distance (r) when exposed to dipoles of a constant size but with greater applied current strengths (I): $\left(E \propto \frac{I}{r^3} \right)$. For example, a shark capable of detecting an electric field intensity of 0.01μV cm^{-1} would encounter that electric field intensity at 14.2cm from the center of the dipole at an applied current of 5.0μA (5.0μA x 1cm = 5μA cm dipole moment). The same electric field intensity would be encountered at 16.6cm at an applied current strength of 8.0μA (8.0μA x 1cm = 8μA cm dipole moment). (This example assumes average testing conditions with a dipole separation of 1cm, a seawater resistivity of

18Ωcm and an orientation angle of 0°) Therefore, increasing the current strength from 5.0μA to 8.0μA would provide only a 17% increase in possible detection distance. The prediction of increased orientation distance at greater applied current strength was not supported by the data. However, the lack of support for this prediction is likely based on the small range of tested electric current strengths. The range of electric currents used in these experiments was chosen based on literature values that had successfully elicited feeding behavior in other elasmobranch species. Consequently, testing was restricted to applied current strengths of 5.0 to 8.9μA. If a greater range of currents had been tested, it might have been possible to detect a difference in orientation distance. However, the prediction of increased orientation distance with increased applied current strength must be qualified by recalling that the nature of the response is dependant on the shark perceiving the stimulus as prey. If the stimulus is not perceived as prey, the shark may detect the electric field but not bite at it. Although the sharks would theoretically respond from a greater distance at higher current strengths, their behavior might modify their response from that predicted by simply scaling the model.

The various combinations of dipole separations and current strengths provided a range of stimuli that jointly affected the orientation distance. For instance, a hypothetical response threshold of 0.01μV cm^{-1}, would occur at 7.93cm for a 1cm dipole separation at 5.0μA of applied current (5.0μA x 1cm = 5μA cm dipole moment). By contrast, that same electric field intensity would occur at 15.87cm for a 5cm dipole separation at 8.0μA of applied current (8.0μA x 5cm = 40μA cm dipole moment). The two extreme stimuli

used in these experiments (5μA, 1cm vs. 8μA, 5cm) provided a theoretical doubling in possible detection range while still remaining within the constraints of prey-simulating stimuli.

Response threshold

It was predicted that the sharks would demonstrate the best response to stimuli that most closely matched their natural prey items. Although a variety of prey items of different sizes are found in the stomach of juvenile hammerhead sharks in Kaneohe Bay, the most common prey items are alpheid shrimp and gobies (Clarke 1971). Both of these prey items are small and are most closely approximated by the 1cm and 3cm dipoles. The sharks demonstrated the lowest response threshold (i.e., greatest sensitivity) when exposed to the smallest dipole size (1cm). This indicates that the juvenile scalloped hammerheads are best "tuned" to a small dipole size, as that most closely represents the size of their natural prey items. It is predicted that as the sharks increase in size throughout ontogeny, they will become better "tuned" to larger dipole sizes that will more accurately represent their correspondingly larger prey.

The behavioral response used as the indicator that the shark had detected the dipole is a conservative estimate of the position at which the shark actually detected the electric field. The electric field intensity at the point where the shark initiated its turn may not be the minimum detectable electric field intensity. The shark may have detected the electric field at a greater distance (i.e., at a lower field intensity) but continued to swim along the same trajectory until it reached a field intensity that triggered a behavioral response such as a change in direction. This behavioral response threshold is the value

quantified in these experiments and may be a conservative estimate of the sharks' sensory capabilities.

This study is the first to determine the minimum response threshold of a sphyrnid shark to electric stimuli. It has been hypothesized that the wider head of sphyrnids might confer greater sensitivity to electric fields based on the longer ampullary tubules (Compagno 1984, Kajiura 2001). Two percent of all orientations by the juvenile scalloped hammerhead sharks were to a stimulus of less than 1nV cm^{-1} and 4.7% of orientations were to a stimulus of less than 2nV cm^{-1}. These values compare favorably with other non-sphyrnid shark species. The smooth dogfish, Mustelus canis, demonstrated the ability to detect voltage gradients as low as 5nV cm^{-1} (Kalmijn 1982, 1988). Trained captive nurse sharks, Ginglymostoma cirratum, demonstrated minimum threshold sensitivities of 5 to 10nV cm^{-1} in the presence of a 20nV cm^{-1} applied background field (Johnson et al. 1984). Thus, it appears that the hammerheads demonstrate a lower response threshold than those other species but this result must be interpreted with caution. Although the experimental apparatus and stimuli used in these experiments were similar to those described by Kalmijn (1978, 1982), differences in analytic methods might not allow the results to be directly compared. For instance, previous studies merely estimated orientation distance and were unable to analyze footage frame-by-frame to determine precise orientation distance. In addition, whereas previous studies grouped orientation angles as either along the dipole axis, normal to the dipole axis or intermediate, this study was able to accurately measure orientation angle to the nearest degree from the video footage. The limitation of different methodologies can

be overcome by testing sphyrnid and non-sphyrnid sharks under identical conditions and comparing the minimum response thresholds obtained for the different species.

These experiments deliberately tested only stimuli that simulated natural prey items. Thus, the range of stimulus size and intensity was limited. However, sharks are capable of detecting non-prey electric fields. Sharks respond to the electric fields of conspecifics (Tricas et al. 1995), of predators (Sisneros et al. 1998) and can theoretically respond to induced fields caused by swimming through the earth's magnetic field (Kalmijn 1974, Paulin 1995) or near geomagnetic anomalies (Klimley 1993). Therefore, there is a wide range of electric stimuli that sharks might detect which remains to be tested.

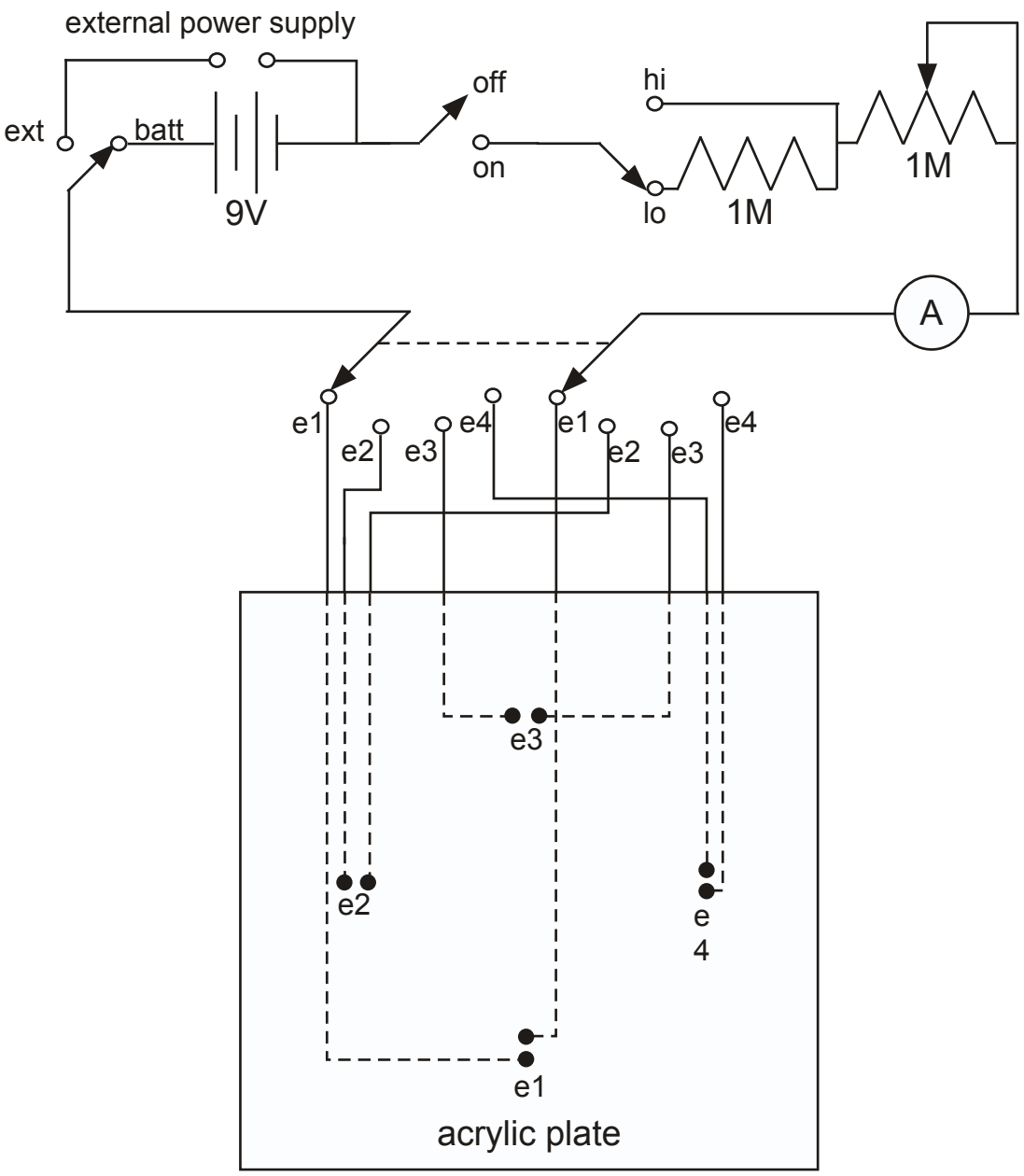

Figure 3.1 Circuit diagram of the stimulus generator used to present prey-simulating dc dipole electric fields in seawater. Current is passed through the seawater at one of four electrode pairs (e1-e4) and a dipole electric field is generated in the seawater around the electrodes. The current is passed to the electrodes on the acrylic plate via underwater cables (not drawn to scale).

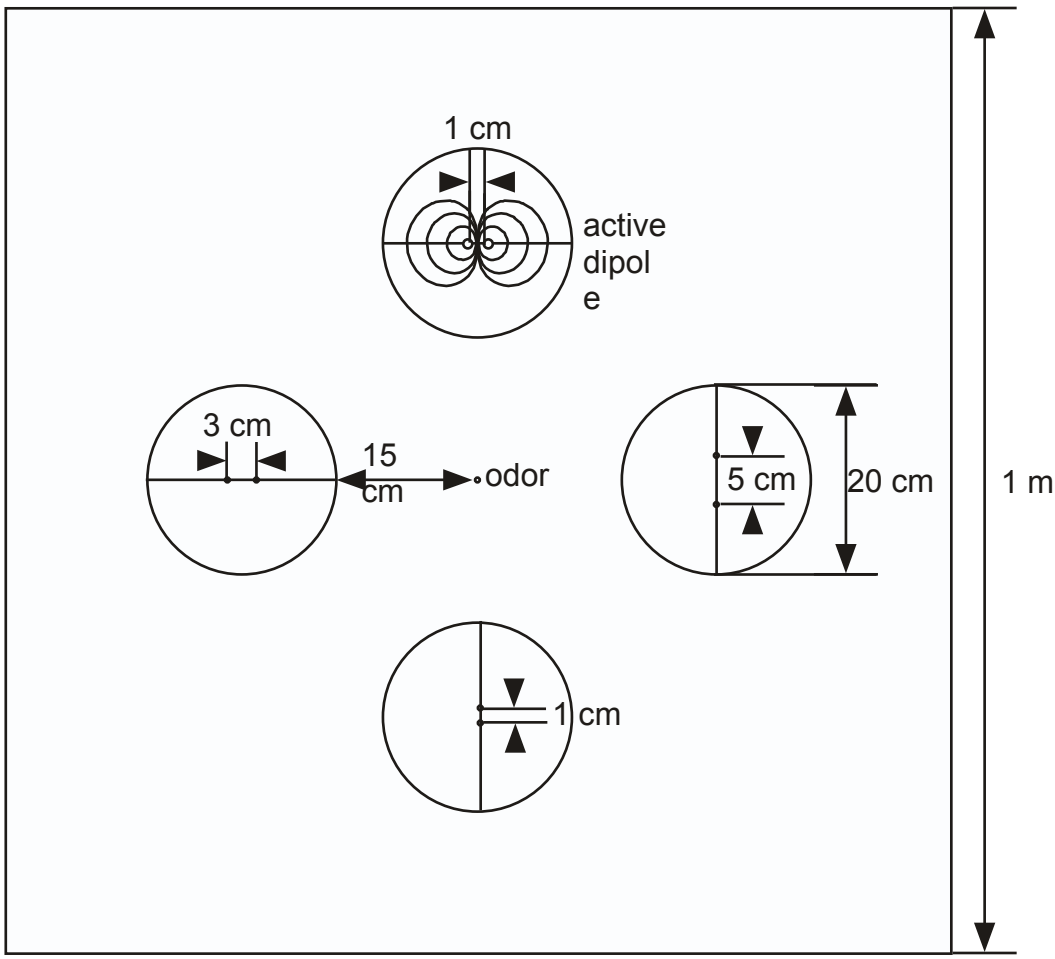

Figure 3.2 Electrode array used to study the response of scalloped hammerhead sharks to prey-simulating dipole electric fields. In each trial, one of the four electrode pairs was activated with a weak electric current which generated a dipole electric field around the electrodes. Electrodes were spaced either 1, 3 or 5 cm apart and each electrode pair was equidistant from an odor delivery tube in the center of the plate. The electrodes were spaced symetrically on the plate and around the center of each electrode pair a 10 cm radius circle was drawn which served as a frame of reference for subsequent video analysis. A line drawn on the plate through the dipole axis was also used in video analysis to reference orientation angle of the shark with respect to the dipole axis.

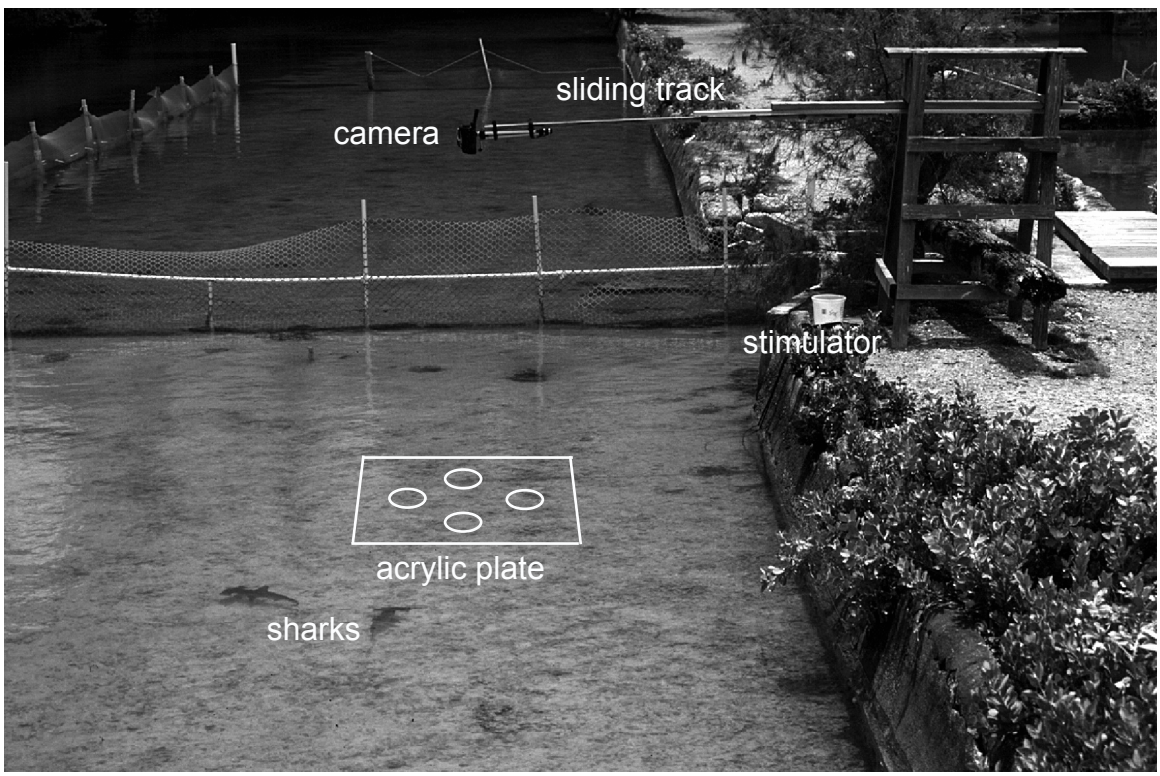

Figure 3.3 Experimental apparatus used to study the response of scalloped hammerhead sharks to prey-simulating dipole electric fields. One of the four electrode pairs (circles on the acrylic plate) was activated with a weak electric current which generated a dipole electric field around the electrodes. The response of the sharks was videotaped with a camera affixed to the end of a sliding track and positioned directly above the center of the electrode array.

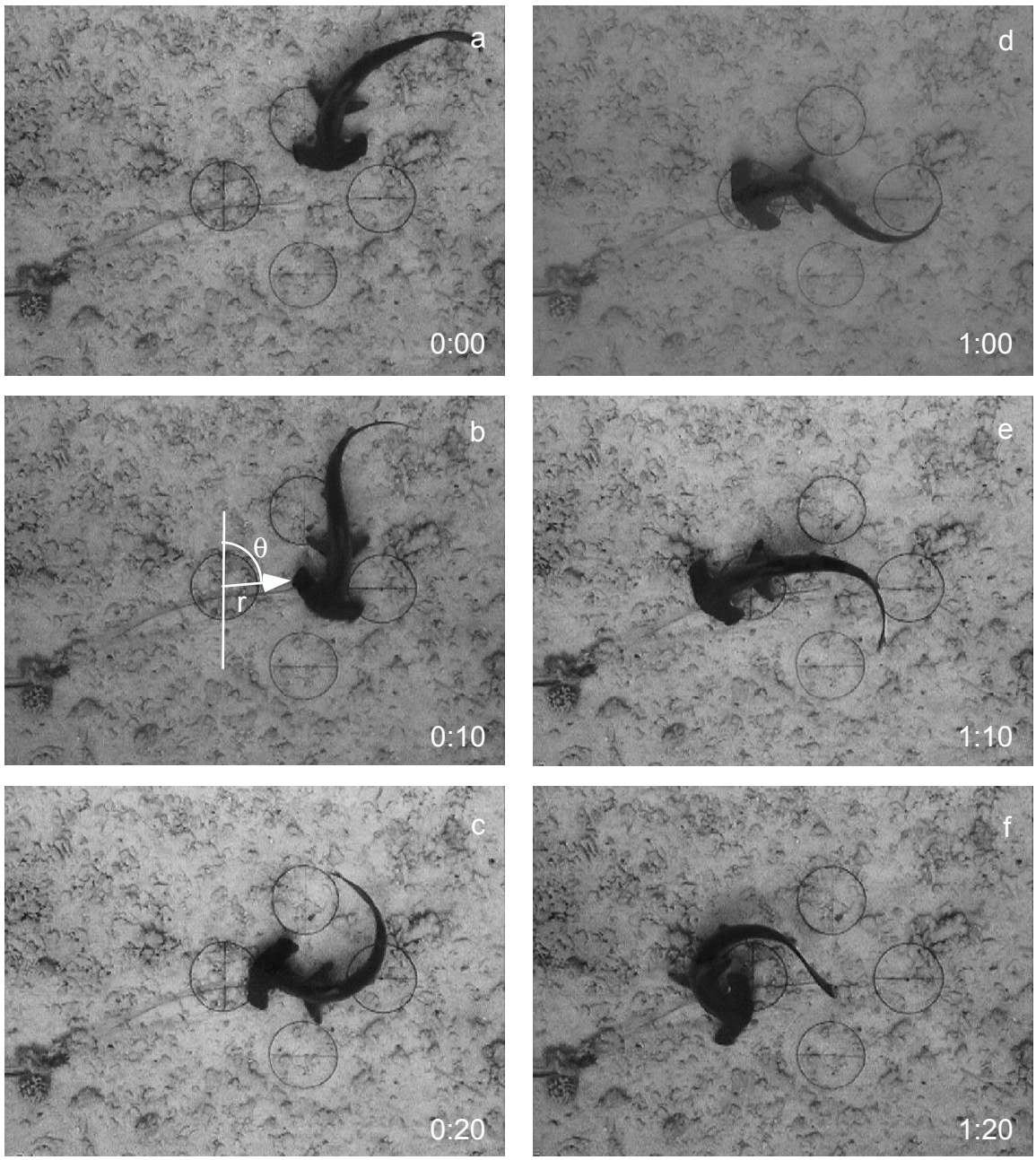

Figure 3.4 Representative sample of a hammerhead shark orientation to a dipole electric field. The shark is (a) swimming within frame prior to detection of the electric field. The shark (b) initiates an orientation to the dipole and the distance (*r*) of the shark with respect to the center of the dipole is measured as well as the angle (θ) with respect to the dipole axis. The shark (c) swims toward the electrodes and (d) bites at the electrodes. After biting, the shark (e) swims away and (f) promptly turns back toward the electrodes. The counter in the lower right of each frame denotes seconds:frames.

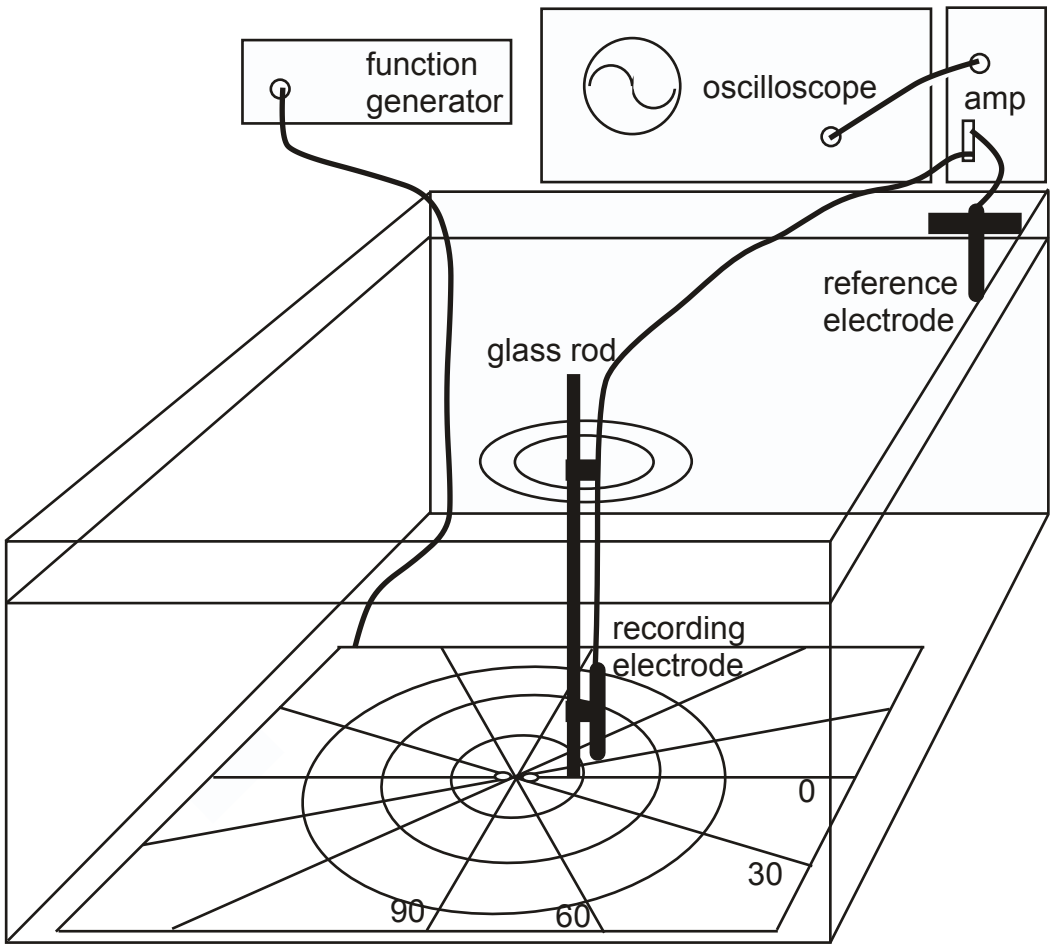

Figure 3.5 Experimental apparatus used to measure voltage in a controlled environment. A function generator produced a 1kHz sine wave in the seawaterthrough the electrodes in the acrylic plate on the bottom of the tank. The voltage was measured differentially with a recording electrode that was moved to various positions around the dipole. Concentric circles of 5, 10, 15 and 20cm radius were drawn around the center of the dipole and lines radiated from the dipole axis at 0º, 30º, 60º and 90º. These landmarks served as reference points to position the recording electrode relative to the center of the dipole. Output from the differential amplifier was observed on the oscilloscope.

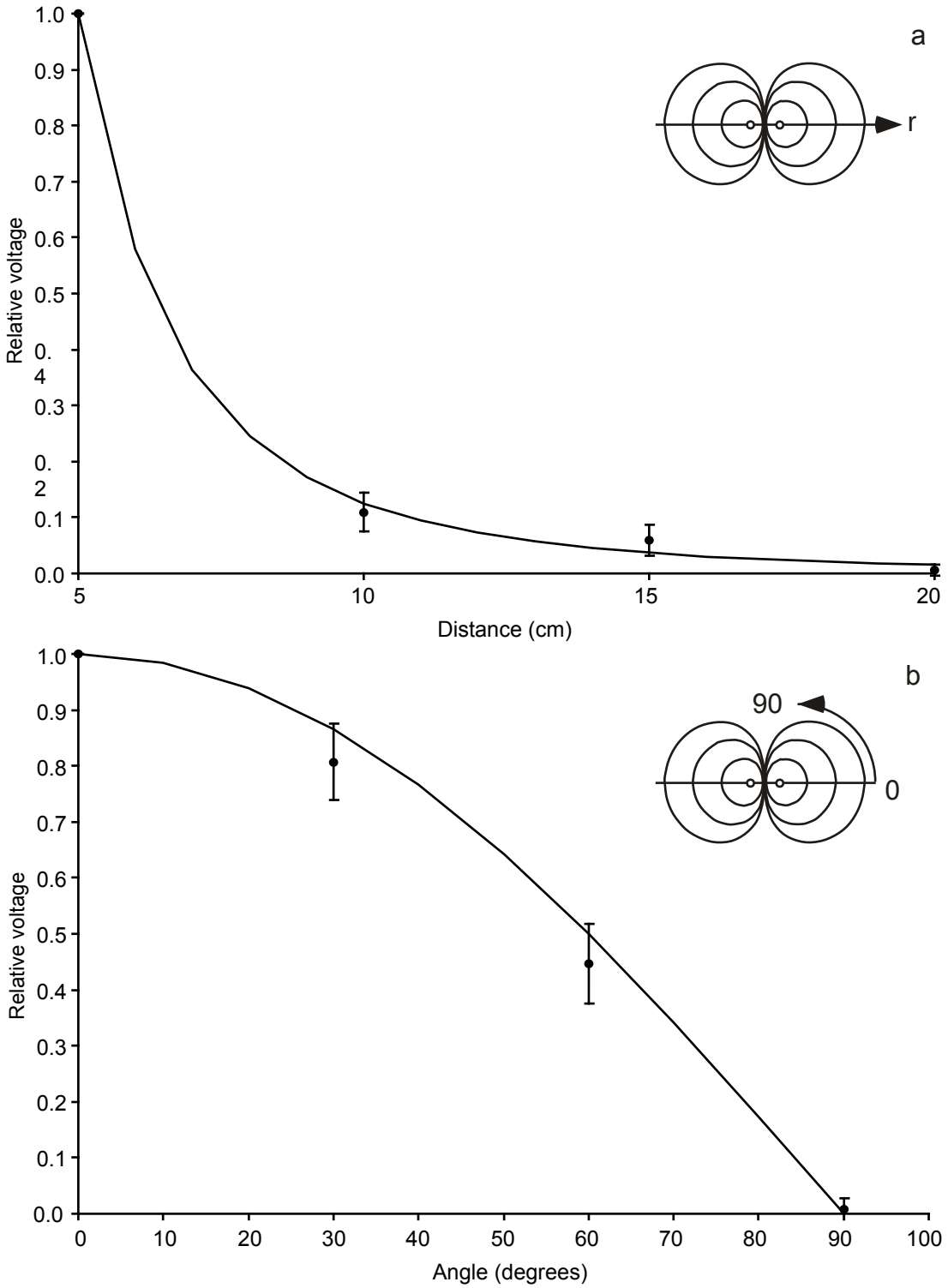

Figure 3.6 Measured values (mean ± SD) of the voltage plotted with the calculated theoretical values. The voltage (a) decreases as a cube of distance and also (b) decreases as a cosine function from a maximum at 0º to a minimum at 90º. The measured values closely match the theoretical values. The data are scaled to a maximum relative voltage of 1.0.

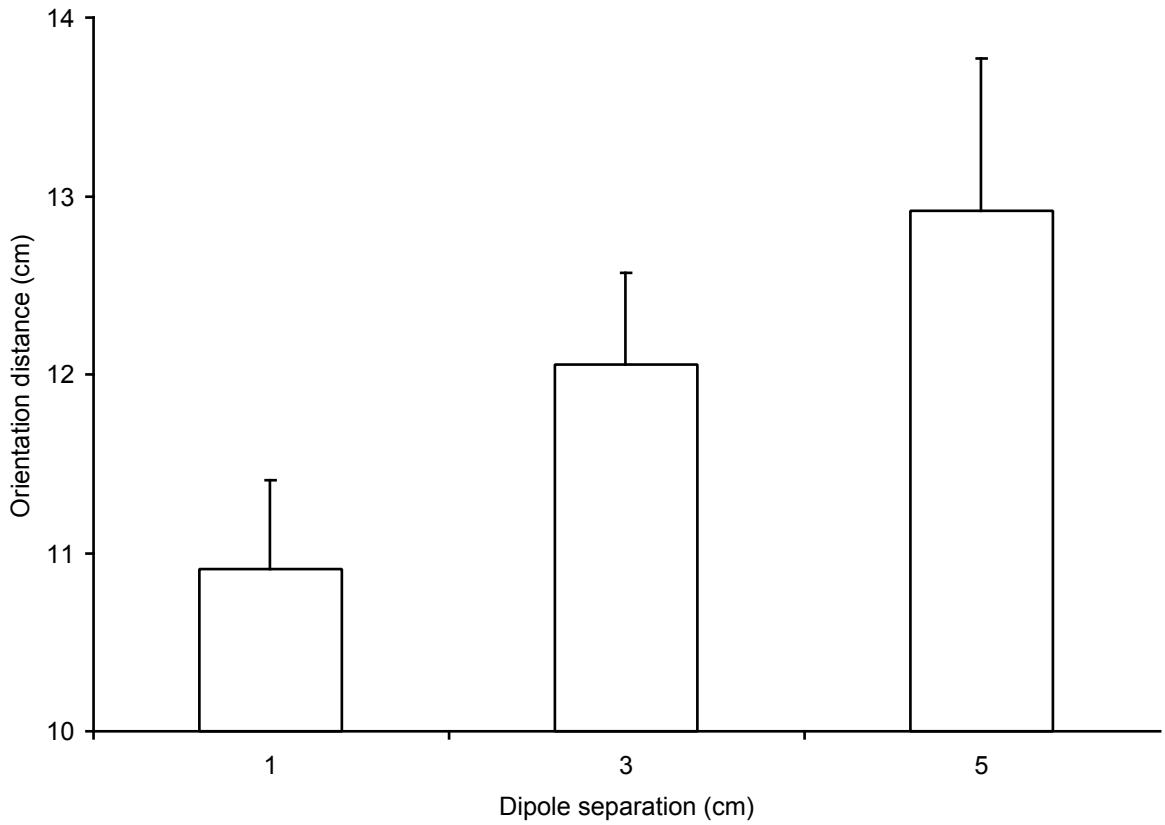

Figure 3.7. Mean orientation distance + SE for three dipole separation sizes. Sharks oriented from greater distances at greater dipole separation sizes. The difference was significant between the 1 and 5cm dipole sizes. Distance was measured from the edge of the shark's head to the center of the dipole.

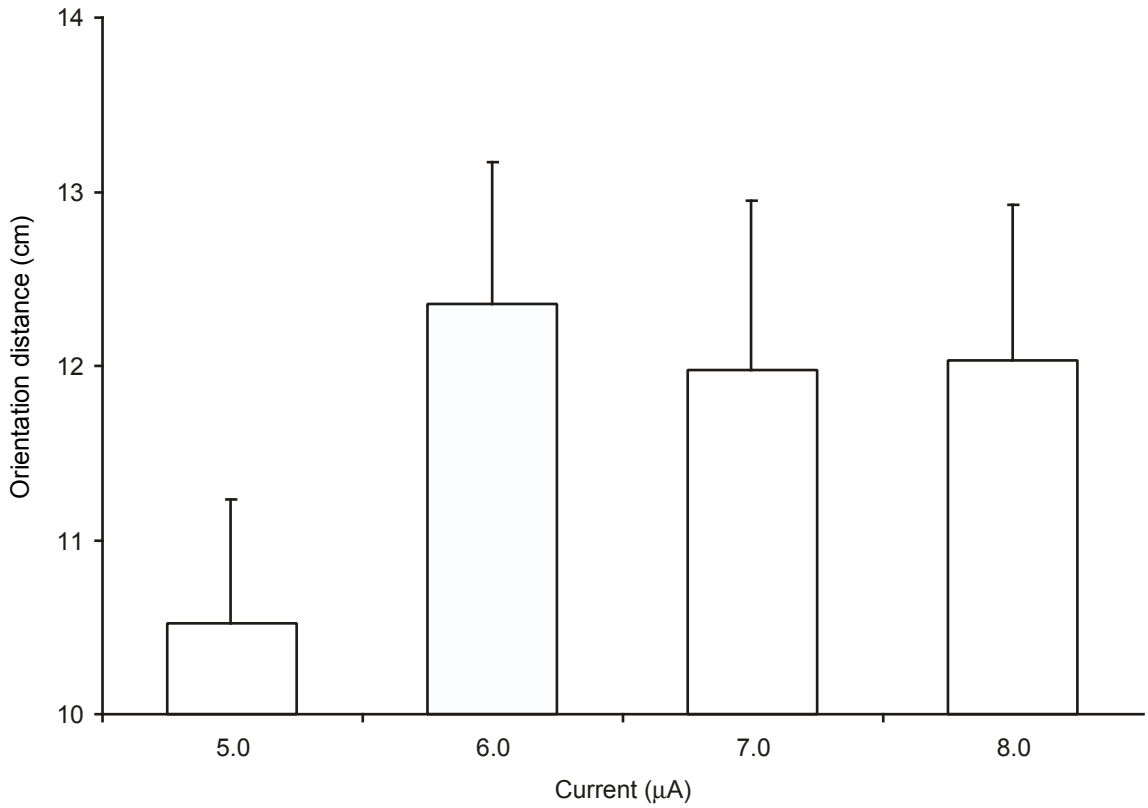

Figure 3.8 Mean orientation distance + SE for four levels of applied electric current. There was no significant difference in orientation distance with increased applied current. Distance was measured from the edge of the shark's head to the center of the dipole.

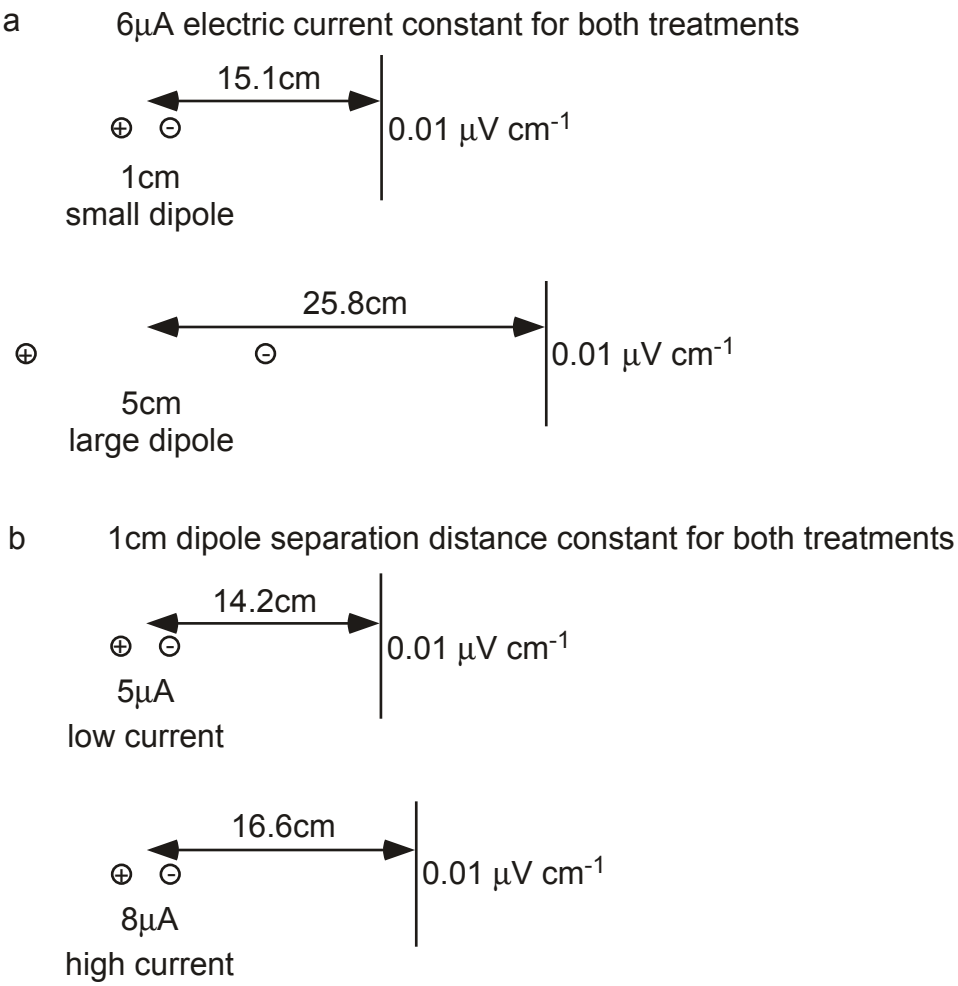

Figure 3.9 Diagrammatic representation of how voltage gradient varies with changes in dipole separation and current strength. Any given voltage gradient ($\mu V\ cm^{-1}$) will occur at a greater distance from the center of the dipole when (a) dipole separation is increased and current strength is constant; or when (b) current strength is increased and dipole separation is constant. In the first example (a), the electric current strength is held constant at 6μA for dipole separations of 1cm and 5cm creating dc dipole moments of 6 μA cm and 30 μA cm respectively. A voltage gradient of $0.01\mu V\ cm^{-1}$ is produced at 15.1cm from the center of a dipole which has a separation of 1cm. That same voltage gradient ($0.01\mu V\ cm^{-1}$) occurs at a distance of 25.8cm from the center of a dipole which has a separation of 5cm. In the second example (b), the dipole separation is held constant at 1cm for applied current strengths of 5μA and 8μA. A voltage gradient of $0.01\mu V\ cm^{-1}$ is produced at 14.2cm from the center of a dipole which has an applied current strength of 5μA. That same voltage gradient ($0.01\mu V\ cm^{-1}$) occurs at a distance of 16.6cm from the center of a dipole which has an applied current strength of 8μA. Both of these examples assume average testing conditions experienced during the trials (seawater resistivity = 18Ωcm, orientation angle = 0º). Distances not drawn to scale.

CHAPTER 4

COMPARATIVE ELECTRORECEPTION IN JUVENILE SCALLOPED HAMMERHEAD AND SANDBAR SHARKS

INTRODUCTION

All elasmobranchs can detect electric fields with their electrosensory system, the ampullae of Lorenzini. In some species this electrosense enables them to locate potential prey items that might otherwise be obscured from their other sensory systems, for example if the prey is buried in the substratum. Although elasmobranch orientation to prey bioelectric fields was first documented over thirty years ago (Kalmijn 1966), surprisingly few studies have since examined the ethology of the behavioral responses of elasmobranchs to potential prey items.

Of more than 380 shark species (Compagno 1999), only eight species have been examined for electroreceptive response (Chapter 1). Of those, the minimum voltage gradients that elicit a feeding response have been determined for only the smooth dogfish, Mustelus canis (Kalmijn 1982) and the nurse shark, Ginglymostoma cirratum (Johnson et al. 1984). No studies have examined the electrosensory-mediated behavioral response of sphyrnid sharks even though it is hypothesized that enhanced electroreceptive capabilities might have driven evolution of the sphyrnid head morphology (Compagno 1984).

The enhanced electrosensory hypothesis holds that the sphyrnid head morphology increases electrosensory search area and maximizes sensitivity to electric fields. Morphological evidence supports this hypothesis. The wider head of sphyrnid sharks provides a greater search area when compared to similar sized carcharhinid sharks

(Chapter 2). The consequent greater head area is accompanied by a greater number of electrosensory pores that provide sphyrnids with a pore density (pores cm^{-2}) comparable with other species. Because the pore density remains comparable, there is no loss of spatial resolution over the width of the head (Chapter 2). However, although there is supporting morphological evidence, a comparison of behavioral responses to electrosensory stimuli between carcharhinid and sphyrnid sharks is lacking.

This study describes and quantifies the behavioral responses of a sphyrnid and a carcharhinid shark to test the predictions of the enhanced electrosensory hypothesis. The response of juvenile scalloped hammerhead sharks, Sphyrna lewini, and sandbar sharks, Carcharhinus plumbeus, to prey-simulating electric fields was compared to determine if scalloped hammerhead sharks demonstrated a greater sensitivity to dipole electric fields than similarly sized sandbar sharks. The area sampled by the sharks as they swim was also quantified to compare effective electrosensory search area between the species. These two species were chosen to respectively represent typical sphyrnid and carcharhinid head morphologies. Comparative behavioral studies of feeding response should test species that share a similar feeding behavior. Juvenile scalloped hammerhead sharks feed primarily on benthic fishes and crustaceans (Clarke 1971). Juvenile sandbar sharks also feed primarily on benthic fishes and crustaceans but also feed on small fishes in the water column (Medved et al. 1984). In addition, both species occur at a comparable size range as juveniles (Compagno 1984). Thus, a comparison can be made between two comparably sized species with somewhat similar feeding habits that differ in head morphology.

METHODS

Capture and holding

Thirteen juvenile scalloped hammerhead sharks, S. lewini, were captured as described in Chapter 3. Fourteen juvenile sandbar sharks, C. plumbeus, were caught by longline fishing on the reef drop-off outside Kaneohe Bay, Oahu (approximately 21° 29.9´N, 157° 46.3´W). Transport of the sandbar sharks to the Hawaii Institute of Marine Biology was via a covered 1.2m diameter fiberglass holding tank and the sharks were maintained in the same outdoor pens as the hammerheads. For both species, sharks were measured, sexed and marked with identifying fin clips prior to being placed in the pen. Sharks were allowed to acclimate for a minimum of one week prior to testing.

Experimental protocol

The experimental apparatus and bioassay protocol were the same as those described in Chapter 3. However, for the purposes of inter-specific comparison, sharks were exposed to only a single stimulus. A 1cm dipole with an applied current of 6.0μA was used in the trials. This stimulus was chosen based on the parameters that elicited the best response for juvenile scalloped hammerhead sharks (Chapter 3). An individual shark was stimulated to search for food by introduction of an odor stimulus. One of four randomly selected electric dipoles was activated for each trial and the response of the shark to the dipole was videotaped with an overhead camera. Several passes and bites at the activated dipoles were recorded for each individual and at the end of a trial, the shark was fed to satiation then starved for two to six days prior to the next trial. Whereas the hammerheads were starved for only two days between trials, the sandbar sharks were

starved for four to six days between trials. The longer starvation period for the sandbar sharks was necessary to enable them to demonstrate a comparable response (i.e., increased tail beat frequency) when exposed to food odor stimulus.

The motivational state of individual sharks was assessed by quantification of their swimming behavior (i.e., tail beat frequency). The number of tail beats in one minute was counted in sharks that were not stimulated by food odor and was counted again after introduction of food odor when the sharks were stimulated to search for food. Tail beat frequency of food odor stimulated and non-stimulated sharks of both species was compared with an ANOVA. Experiments were conducted with relatively naive sharks that had not been exposed to the activated dipoles for more than three trials.

Video analysis

The video footage was digitized and analyzed as described in Chapter 3. Frame-by-frame analysis allowed detailed observation of the orientation pathways of the sharks. Various orientation pathways were described and the frequency of occurrence of each was compared between species. The frame in which a shark first demonstrated a turn toward the dipole (i.e., orientation) was extracted and analyzed with image analysis software (NIH Image v1.6.1). A subsample of 25 randomly selected orientation events for each species was analyzed to quantify the course deviations. A turn toward the dipole was defined as a deviation of greater than 20° from the swimming trajectory of the shark immediately preceding the turn. The distance and angle with respect to the dipole axis were measured and used to calculate the electric field intensity (voltage gradient) at the point where the shark initiated its turn (Chapter 3). The calculated field intensity values

were log transformed to apply general linear models and compared between the two species.

The probability of the head of a shark passing over the center of a 1cm^2 dipole was calculated for all possible straight trajectories across the field of view of the video camera (~ 99 x 132cm). The maximum probability of encounter was compared to the rate of encounter for the orientations.

Search area

Search area was defined as the area immediately under the head of the shark and was quantified by analyzing the swimming path of sharks as they swam in the absence of introduced olfactory stimuli. Ten individuals of each species were videotaped as they swam in a slow, steady, straight trajectory under the camera mounted on the sliding track over the shark pen. Digital movies were created of each pass and analyzed on the computer by marking points over each eye for every other frame of a one second sequence (Figure 4.1). A polygon was created by connecting each point and the area of the polygon was calculated by calibration of the image analysis software to a known measurement within the field of view. The area sampled by the head of the shark was thus quantified and compared between the two species using a t-test for unequal variances.

A similar technique was used to quantify the velocity of the sharks. The linear distance traveled by the shark in a one second period was measured and compared between the species using a t-test.

Torso flexibility

The maximum lateral flexure demonstrated by scalloped hammerhead and sandbar sharks as they turned toward a dipole electric field was measured by digital video analysis. The video frame in which the shark demonstrated the greatest body flexure toward the dipole was analyzed for six individuals of each species. Lines were drawn from the center of the snout to the origin of the first dorsal fin and then to the dorsal precaudal notch on the caudal peduncle. The resulting angle was measured for each individual, the data were pooled within the two species and analyzed with an ANOVA.

The degree of flexibility is at least partly attributable to the cross sectional area of the trunk. To measure cross sectional area, the heads of 14 scalloped hammerhead and 13 sandbar shark individuals from a wide variety of sizes were severed in the transverse plane at the posterior edge of the lower jaw. The severed trunk of each head was placed on a piece of paper and the trunk area was traced. The trunk area was digitized and measured with image analysis software (NIH Image v1.61) and the data were analyzed with an ANCOVA.

RESULTS

Both species demonstrated a feeding response by biting at the active dipole and ignoring the non-active dipoles. Sharks sometimes bit repeatedly at an active dipole but immediately stopped biting when the electric current was turned off. Although the hammerhead sharks always responded by biting at the active dipole, the sandbar sharks would occasionally not bite even when they passed within 10cm of the electrodes. These "no bite" responses accounted for 13.3% of the total passes. Only responses in which a

clear orientation (> 20° change in course trajectory) or bite was seen were included in subsequent analyses.

Orientation distance and angle

The primary variate in all behavioral studies of electroreception is the distance from the center of the dipole at which a shark initiates its orientation. Both species initiated orientations from the same range of distances (Figure 4.2). The hammerheads demonstrated the greatest number of orientations from less than 5cm with a maximum orientation distance of 30.6cm. The sandbar sharks demonstrated the greatest number of orientations from less than 10cm and orientated from a maximum distance of 31.6cm. For both species, the orientations from close range were probably not indicative of the maximum sensitivity of the shark because some orientations were initiated from much greater distances at much lower electric field intensities.

If taken in isolation, the distance from the electrodes at which the orientation is initiated is an insufficient indicator of the electric field intensity to which the shark responds. The electric field intensity not only decreases as a cube with increasing distance, but also varies as a cosine function with respect to the dipole axis (Chapter 3). The electric field intensity is greatest in the plane parallel to the dipole axis and decreases to a theoretical null in the perpendicular plane. It was hypothesized that sharks would initiate orientations at a greater distance from low axis angles where the voltage gradient is greatest. This hypothesis was supported by the data. Both species demonstrated a significant inverse relationship between orientation distance and angle with respect to the dipole axis (Figure 4.3; Regression, S. lewini $F_{1,57} = 4.715$, $p = 0.0342$; C. plumbeus $F_{1,35}$

= 20.376, $p < 0.0001$). That is, both species initiated orientations from a greater distance at low axis angles. To detect the same electric field intensity, the sharks needed to be closer to the dipole when they encountered the field at angles near 90°. The initial angle of encounter with respect to the dipole axis did not differ from a random distribution for either species (Regression, S. lewini $F_{1,8} = 3.329$, $p = 0.1108$; C. plumbeus $F_{1,8} = 0.615$, $p = 0.4587$). That is, the sharks initiated orientations from all around the dipole. Therefore, although the sharks initiated orientations from all around the dipole they oriented from a greater distance when they initiated orientations from small axis angles.

Behavioral response threshold

The electric field intensity was calculated from the position at which the shark initiated its orientation to the dipole. This electric field intensity value was defined as the response threshold. Both species initiated approximately 70% of orientations at an electric field intensity of less than 0.1 $\mu V\ cm^{-1}$ (Figure 4.4). The percentage of orientations at higher electric field intensities decreased markedly for both species. Data from orientations to an electric field intensity of less than 0.1 $\mu V\ cm^{-1}$ are shown in Figure 4.5. The frequency distribution of orientations was remarkably similar for the two species with both species initiating approximately 35 to 40% of all orientations to an electric field intensity of less than 0.01 $\mu V\ cm^{-1}$. Because of the strongly skewed distribution of the behavioral response threshold values, median values rather than means were compared between the two species (Sokal & Rohlf 1981). The median behavioral response threshold for the hammerhead sharks was 0.0252 $\mu V cm^{-1}$ and for the sandbar

sharks was 0.0303 μVcm^{-1}. The log transformed median values did not differ between the species (ANOVA, $F_{1,119} = 0.014$, $p = 0.9064$) which indicates that the hammerhead sharks did not demonstrate greater sensitivity than the sandbar sharks to dipole electric fields.

Behavioral response

The motivational state of the sharks was assessed by counting the tail beat frequency of individuals prior to and subsequent to the introduction of a food odor stimulus. In the absence of introduced olfactory stimuli, the sharks swam in a slow, steady, relatively straight trajectory. In contrast, when exposed to a food odor stimulus, both species demonstrated a marked change in swimming behavior characterized by an increased tail beat frequency and more frequent changes in swimming trajectory. The scalloped hammerheads had a significantly higher tail beat frequency than the sandbar sharks in both food odor stimulated (ANOVA, $F_{1,18} = 11.436$, $p = 0.0033$) and non-stimulated states (ANOVA, $F_{1,30} = 11.138$, $p = 0.0023$). However, both species demonstrated a similar and significant relative increase in tail beat frequency from non-stimulated to stimulated states (S. lewini: 1.76x, C. plumbeus: 1.61x).

Although both species bit at the dipole, the characteristic orientations to a stimulus differed. The hammerheads typically responded by swimming within detection range of the dipole, then turning sharply toward the dipole. A subset of 25 randomly selected orientation events demonstrated a mean turn angle of 101.0°±4.56SE with a minimum of 41.1° and a maximum of 137.3° for the hammerhead sharks. The sandbar sharks demonstrated a mean turn angle of 68.5°±4.97SE with a minimum of 23.9° and a

maximum of 120.7°. In the process of executing a turn, the hammerheads appeared to pivot in position with the side of the head that was closest to the dipole remaining nearly stationary relative to the center of the dipole while the body bent into a C shape. In contrast, the sandbar sharks oriented toward the dipole by swimming in a broader arc that eventually brought them to the center of the dipole. Although the swimming behavior of the two species differed, several distinguishable orientation patterns were recognized in both species (Figure 4.6).

Single turn

The "single turn" was by far the most common type of orientation and accounted for over half of all orientations for both species. As the shark was swimming within the field of view of the videocamera it made an abrupt turn (> 20° change in course trajectory) and changed course to bring its head directly to the center of the dipole which it then bit. The distance of orientation was measured from the center of the dipole to the point at which the shark initiated its turn toward the dipole (Chapter 3). The edge of the head closest to the electrodes was chosen as the point of reference on the shark. No part of the shark's body was over the electrodes when the shark initiated its turn. A "single turn" was, by definition, only one change in trajectory with no subsequent course correction required to position the shark's head over the center of the dipole.

Straight

A "straight" approach was described as the shark swimming into the field of view of the video camera on a trajectory that brought any part of its head directly over the active dipole. The shark would abruptly stop and bite at the active dipole. Because there was no change in trajectory (only minor swimming movements of <20°), it was

impossible to determine at what point the shark first detected the field. Therefore, no value could be ascribed to the electric field intensity that initiated a response. Included within the "straight" approach was the "pivot" exhibited by the hammerheads. This approach was defined as a lateral extension of the cephalofoil passing directly over the electrodes and the shark turning toward the electrodes while keeping in position the part of the head already over the electrodes. The shark would thus appear to pivot with the side of the head over the electrodes seeming to remain fixed in position. Thus, a "straight" approach was characterized by a trajectory that brought the shark from out of frame over the center of the dipole with no change in course. "Straight" approaches were seen in approximately a third of all passes for both species.

The maximum probability of encountering a $1cm^2$ dipole on a straight trajectory across the field of view of the video camera is 0.2325. This value is much lower than the rate of encounter for the hammerhead sharks of 0.339 and for the rate of encounter for the sandbar sharks of 0.377.

Overshoot

Overshoot was seen in highly motivated sharks that were swimming very fast. Sharks would sometimes swim straight over the electrodes without biting then quickly double back and bite at the electrodes. An "overshoot" orientation would appear initially as a "straight" approach in which any part of the shark's head passed directly over the electrodes without initiating a bite. Once the shark had swum past the electrodes, it would then turn sharply and double back to bite at the active dipole. The shark would experience increasing electric field intensity as it swam over the dipole and the field intensity would decrease as the shark moved past the dipole. It was presumed that the

shark turned back toward the electrodes at the point where it failed to detect the electric field. The maximum distance of the head past the electrodes was quantified for the "overshoot" response. This response was seen in 11.3% of orientations for the hammerheads and 7.5% of orientations for the sandbar sharks.

Spiral tracking

A "spiral tracking" orientation occurred when the shark made a series of turns in the same direction that brought it to the center of the dipole through a spiral pattern. This is distinct from the "single turn" orientation in which only one turn was made to bring the shark directly to the center of the dipole. The distance of orientation was measured from the point at which the shark first turned toward the electrodes. The "spiral tracking" orientation typically described a path that followed the curvature of the electric field lines to the center of the dipole. "Spiral tracking" was seen in only 4.0% of orientations for the hammerheads and was not seen in the sandbar sharks.

Search area

The area of the substratum sampled by the head in one second was quantified for ten individuals of each species. The search area was quantified for individuals across a small (~ 10cm) size range for both species. The search area did not differ significantly with size (TL) of the sharks for either species (Figure 4.7; Regression, S. lewini $F_{1,9}$ = 1.359, p = 0.2774; C. plumbeus $F_{1,9}$ = 1.995, p = 0.1955). Because there was no difference in search area across the range of tested sizes, the search area data were pooled and compared between the species with a t-test. The mean search area for the hammerhead sharks was 677.8 cm^2 s^{-1} and for the sandbar sharks was 298.0 cm^2 s^{-1}.

Although the hammerhead individuals were significantly smaller than the sandbar sharks (t-test, $t_{18} = 5.392$, $p < 0.0001$) they sampled a greater area of the substratum per unit time than the sandbar sharks (t-test for unequal variances, $t_{18} = 8.619$, $p < 0.0001$). The hammerhead sharks demonstrated a mean velocity of 37.6 cm s^{-1} and the sandbar sharks demonstrated a mean velocity of 38.5 cm s^{-1}. There was no difference in velocity between the two species (t-test, $t_{14} = -0.348$, $p = 0.7316$).

Flexibility

The maximum body flexure was quantified for individuals of both species as they turned toward the dipole. Hammerheads displayed a mean maximum flexure angle of 85.9° whereas sandbar sharks displayed a mean maximum angle of 113.3° (Figure 4.8). Hammerheads were able to bend at a significantly more acute angle than the sandbar sharks (t-test, $t_{43} = 7.083$, $p < 0.0001$). This difference in flexibility is partially attributed to the cross sectional area of the trunk. The sandbar sharks had a significantly greater trunk cross sectional area than the hammerhead sharks across a wide range of sizes (Figure 4.9; ANCOVA, $F_{1,23} = 14.134$, $p = 0.001$).

DISCUSSION

This study is the first to compare behavioral responses to prey-simulating bioelectric fields in two shark species in order to test the predictions of the enhanced electrosensory hypothesis. The enhanced electrosensory hypothesis predicts that hammerhead sharks will demonstrate greater sensitivity to electric fields and will sample a greater area of the substratum than comparably sized carcharhinid sharks. These

predictions were tested under the semi-natural conditions of the shark pens at the Hawaii Institute of Marine Biology. An advantage to using the outdoor pens to conduct the experiments is that the environmental parameters and benthic infauna are similar to those encountered by the sharks under natural foraging conditions. Therefore, the behavioral responses observed in the pens are likely representative of natural responses in the wild.

Sensitivity

The first prediction of the enhanced electrosensory hypothesis is that the scalloped hammerhead sharks should demonstrate greater sensitivity to electric fields than similar sized sandbar sharks. This prediction is based on the morphology of the electrosensory system within the laterally expanded sphyrnid cephalofoil. The wider head allows sphyrnids to possess longer ampullary tubules (see Chu & Wen 1979) which will confer greater sensitivity to electric fields (Murray 1974; Bennett & Clusin 1978; Tricas 2001). This study determined behavioral response threshold (i.e., sensitivity) by calculation of the minimum electric field intensity that elicited a behavioral response by the sharks. Both species demonstrated similar behavioral response thresholds with median responses from 0.025 to 0.030 μVcm^{-1}. The failure to detect a difference in sensitivity between the two species does not necessarily indicate that there is no difference between the two species; "Absence of evidence is not evidence of absence."

These current experiments failed to demonstrate a difference in sensitivity to a dipole electric field but the hammerheads might demonstrate greater sensitivity than the sandbar sharks to other types of electric stimuli. If the sharks are exposed to a large, uniform electric field, a difference in sensitivity might be detected. In a uniform field the

ampullary cluster is exposed to a voltage potential that is different from the voltage at the pore openings and hence, longer tubules will sample a greater voltage gradient and will result in greater sensitivity (Kalmijn 1988). In contrast, the electric field intensity of a small dipole distant from the head decreases too steeply to affect the potential of the ampullary cluster inside the head of the shark (Kalmijn 1988; Tricas 2001). Although the two species did not demonstrate a difference in sensitivity to the small, prey-simulating dipole fields, it is predicted that the hammerheads will demonstrate greater sensitivity than the sandbar sharks when exposed to large uniform fields.

Over 40% of the orientations for both species were to very low electric field intensities ($<0.02\mu Vcm^{-1} = 20nVcm^{-1}$), which indicates that both species detect and respond to extremely weak electric fields. The behavioral response threshold for both species closely matches that obtained by recording from the primary afferent neurons in the electrosensory system of the round ray, Urolophus halleri, (Tricas & New 1998) which encodes electrosensory information down to $20nVcm^{-1}$.

The behavioral response threshold may differ as a function of motivational state. A highly motivated shark may demonstrate a lower response threshold (i.e., greater sensitivity) than a shark that is not aroused or hungry. Because the swimming velocity was the most obvious change in behavior after introduction of food odor, tail beat frequency was used as a measure of motivation. For both species, the tail beat frequency of sharks stimulated by food odor was approximately 1.6 to 1.7x the tail beat frequency of non-stimulated sharks. The sandbar sharks had to be starved for much longer than the hammerheads to achieve this similar increase in tail beat frequency. If the tail beat frequency is not a comparable measure of motivation between the species, one species

might have been more highly motivated than the other. Although it was predicted that the hammerhead sharks would demonstrate greater sensitivity to electric fields, this prediction was not supported by the data. If the sandbar sharks were more highly motivated, they might have responded to lower electric field intensities and thus appeared to demonstrate equal sensitivity to the hammerheads. The use of a different motivational state indicator, for instance stomach pH, might reveal that the sandbar sharks were hungrier and thus responded more readily than the hammerheads thus giving the sandbar sharks apparently equal sensitivity.

Orientation pathways

The diversity of orientation pathways indicates that the response of the sharks to electric fields is more varied than previously reported. Previous work simply states that sharks respond with a turn toward the active dipole (Kalmijn 1971, 1978, 1982; Johnson et al. 1984). The ability to analyze responses frame by frame contributes additional details to the types of orientation patterns.

Approximately one third of all bites at the dipoles were the result of "straight" approaches from out of frame. The maximum probability of encountering a given dipole along a straight trajectory is 0.2325. The disproportionate number of "straight" approaches (S. lewini: 0.339, C. plumbeus: 0.377) may indicate that the sharks initiated orientations from outside the field of view of the video camera and swam in a straight trajectory toward the center of the dipole. Attempts were made to eliminate this problem by having the field of view be large (~ 99 x 132cm) with respect to the maximum orientation distance (~ 30cm). Nonetheless, because the field of view of the videocamera

was somewhat variable (depending on extent of zoom) and because the electrode array was not always centered in the field of view, it is conceivable that some orientations might have been initiated from outside the field of view.

The "straight" approach was unable to provide information about the point at which the shark detected the electric field. The shark could have detected the field at any point along its path, but, as there was no obvious change in trajectory, the point at which the shark detected the field remains unknown.

In the "overshoot" orientation, the shark moved past the stimulus until the shark was presumably outside the detection range then abruptly turned, doubled back to the dipole and bit at it. Why the sharks passed over the stimulus without stopping is unclear. It might be that the sharks were simply moving at such a great velocity that their pliant pectoral fins were unable to provide sufficient deceleration to allow them to stop directly over the stimulus. Alternatively, perhaps the sharks were unable to determine the position of the center of the dipole until they had moved past it and detected the inverse field polarity.

The "spiral tracking" is perhaps the most interesting orientation pathway as the hammerheads appeared to follow the direction of current flow toward the center of the dipole. This pathway would be generated if the shark swims to maintain a constant angle with respect to the direction of the electric field which would thus bring the shark to the center of the dipole (Kalmijn 1997). Freshwater electric fishes align their bodies parallel to lines of current flow and, by maintaining this alignment, swim to the center of an electric dipole (Schluger & Hopkins 1987; Davis & Hopkins 1988). Similar orientation behavior is seen in the sculpin in which the lateral line is used to orient to and follow

dipole pressure flow lines of a vibrating sphere (Coombs & Conley 1997). In each of these examples, the orientation path follows along current (or pressure) flow lines and it is reasonable to suggest that sharks are capable of the same type of orientation.

Orientation mechanisms

Two mechanisms have been proposed to explain the ability of the sharks to accurately orient to the center of an electric dipole (Kalmijn 1997). It is possible that the sharks may use both methods to localize the source of the electric field. Once the shark detects an electric field it could orient to the source by following changes in the direction of the field or by analysis of the field configuration (Kalmijn 1997). If the sharks respond only to changes in the direction of the field and swim to maintain a constant angle with respect to the field, they would arrive at the center of the dipole (Kalmijn 1997). Although this is not the most direct path it does describe the "spiral tracking" pattern of orientation exhibited by the hammerhead sharks. Alternatively, the sharks might analyze the field configuration to derive the location of the dipole source (Kalmijn 1997). This would necessitate the shark being able to sample the field differentially across the head. If differential sampling is utilized, the electroreceptors spaced over a greater area on the laterally expanded sphyrnid cephalofoil may provide increased spatial resolution compared to similar sized sharks of other families. Whereas a sphyrnid shark would be better able to detect a voltage gradient across the width of the cephalofoil, a carcharhinid shark, with an electroreceptor distribution laterally constrained by its head morphology, would not be able to sample as great a gradient. Regardless of head morphology, spatial analysis of an electric field is feasible only when the shark is well

within detectable range of the dipole and might be a secondary approach strategy after the shark initially orients based on the direction of the field (Kalmijn 1997). Although the "single turn" orientation is best explained by the shark deriving the location of the dipole by differential sampling across the head, the "spiral tracking" can be explained by the shark following the direction of the field to arrive at the center of the dipole. Therefore, the current results provide partial support for both mechanisms hypothesized by Kalmijn (1988, 1997). However, sharks may possess multiple techniques for localization of electric dipole sources.

Flexibility and maneuverability

Although both species demonstrated similar responses to the dipole electric field, the sandbar sharks exhibited a more limited repertoire of orientation pathways. Whereas the hammerheads demonstrated four different orientation pathways to a dipole (Figure 4.6), the sandbar sharks failed to demonstrate the "spiral tracking" orientation. The absence of this orientation pathway may be attributed to the morphology of the two species. The hydrodynamic properties of the sphyrnid cephalofoil confer greater maneuverability by decreasing stability (Nakaya 1995). The cephalofoil thus enables sphyrnids to turn more quickly and sharply than is possible for a carcharhinid shark.

A second factor that might limit the maneuverability of a sandbar compared to a hammerhead shark is the cross sectional area of the trunk. Whereas hammerheads have a greater head width than comparably sized sandbar sharks (Chapter 2), they also have a smaller trunk cross sectional area (Figure 4.8). This small trunk area may enable the

hammerhead sharks to bend laterally more easily which will manifest itself in greater maneuverability and thus a potentially larger repertoire of orientation behaviors.

The hammerheads demonstrated a smooth gradation of decreasing frequency of orientations at increasing distances (Figure 4.2). However, the sandbar sharks demonstrated a distinct peak at a distance of 5 to 10cm. This peak might be attributable to the differences in trunk flexibility of the two species. The smaller cross sectional trunk area and greater flexibility of the hammerheads enabled them to achieve an acute angle of flexure that was significantly different from the obtuse angle demonstrated by the sandbar sharks (Figure 4.8). This flexibility, coupled with the hydrodynamic properties of the cephalofoil, combined to allow hammerheads to orient to a stimulus even from very close range. In contrast, the stiffer-bodied sandbar sharks were unable to orient as well from close distances because they were unable to bend with the same degree of flexibility as the hammerheads. This difference in flexibility would account for the smaller number of orientations from very close range for the sandbar sharks (Figure 4.2).

Search area

The second prediction of the enhanced electrosensory hypothesis is that sphyrnid sharks will sample a greater area than similar sized carcharhinids. This prediction was tested by quantifying the swath of substratum covered by the head of the sharks as they swam slowly under the video camera. Because the velocity of the two species did not differ, differences in search area can be attributed to the greater head width of the hammerhead sharks (Chapter 2). Although the tested hammerheads were significantly smaller than the sandbar sharks, they sampled a significantly greater area of the

substratum per unit time. The greater head width of the hammerheads more than compensated for their smaller size. If sharks of similar total length had been available for comparison, the difference between species would have been even greater. For example, based on the results from this study, a 60cm TL hammerhead shark would sample an area of 6018.2m^2 in 24h. In contrast, a 60cm TL sandbar shark would sample an area of only 2194.9m^2 in 24h. Therefore, the wider head of the hammerhead shark greatly increases the amount of substratum sampled thus increasing the probability of prey encounter. Thus, the second prediction of the enhanced electrosensory hypothesis is supported.

Although the search area was quantified as the area immediately under the head of the shark (Figure 4.1), the current data indicate that the actual detection range of a prey-simulating electric dipole extends for up to 30cm laterally from the edge of the head for both species (Figure 4.2). Therefore, the effective search area is much greater than the conservative value calculated for the two species.

Additional study

This study examined electroreception in juveniles of both species. For both species, individuals were free living in the natural environment for an undetermined period before being captured and tested. They had thus been exposed to a suite of naturally occurring bioelectric fields and had no doubt used detection of these fields in their feeding behavior. Future studies could examine the electrosensory response of neonatal sharks born in a captive environment in which they were not exposed to any electric fields prior to testing. Their response to prey-simulating fields could then be

examined to determine if the bite response is innate or part of a learning process in which they learn to associate electric fields with prey.

Additional studies could also examine the response of other sphyrnid species with different head morphologies. The slightly expanded head of the bonnethead shark, Sphyrna tiburo, combined with the wider trunk and presumably stiffer body would cause it to respond in a manner intermediate between the scalloped hammerhead and the sandbar shark. At the other morphological extreme within the Family Sphyrnidae is the winghead shark, Eusphyra blochii, which possesses a greatly laterally expanded cephalofoil. It is predicted that the morphology of this species will enable it to demonstrate the greatest sensitivity and highest level of flexibility and maneuverability of all the sphyrnids.

Additional studies could also examine the response of sharks to large, uniform electric fields in which the longer ampullary tubules of sphyrnids should confer greater sensitivity. Therefore, a large number of additional factors remain to be considered and studied in the field of elasmobranch electroreception.

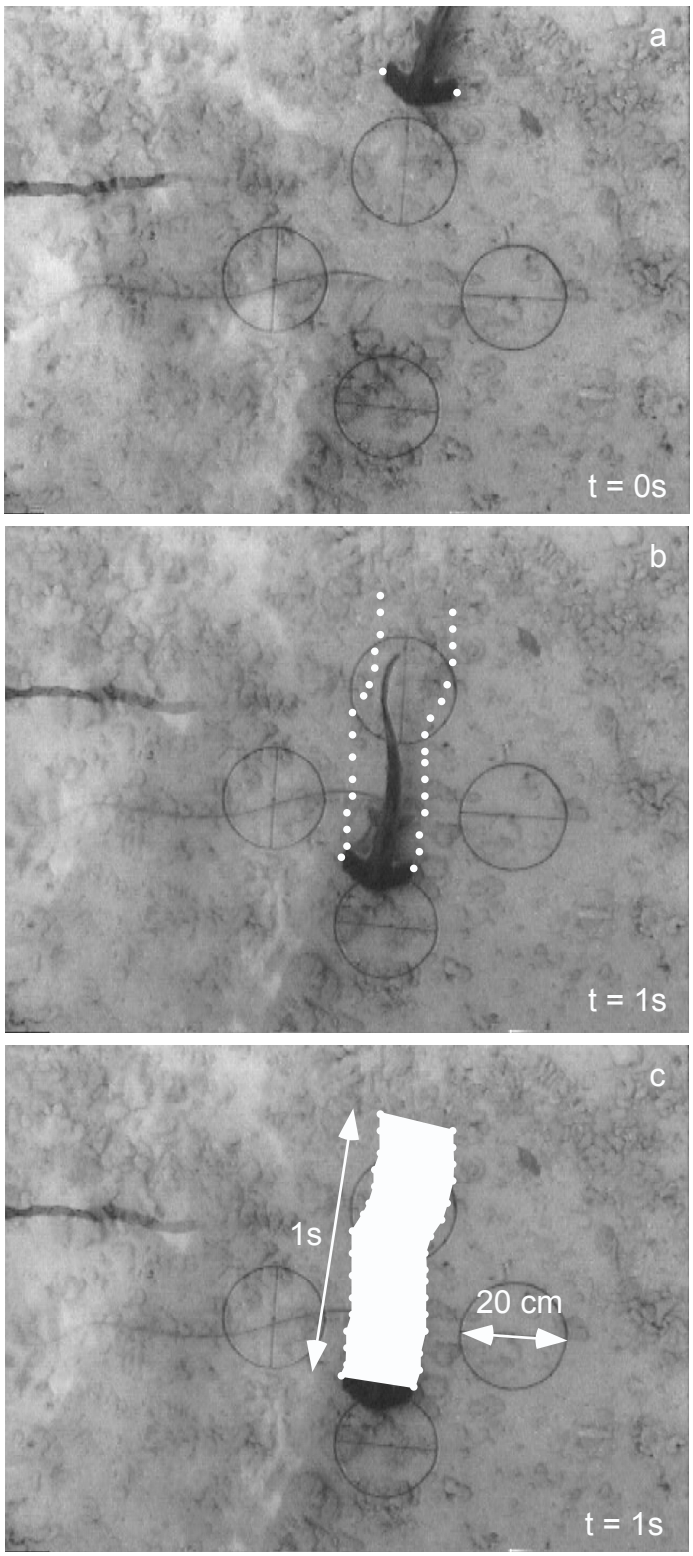

Figure 4.1 Search area quantification. The positions of the distal extremes of the head were marked at every other frame for a one second period. The area that the head had covered in that one second period was measured by reference to a known area.

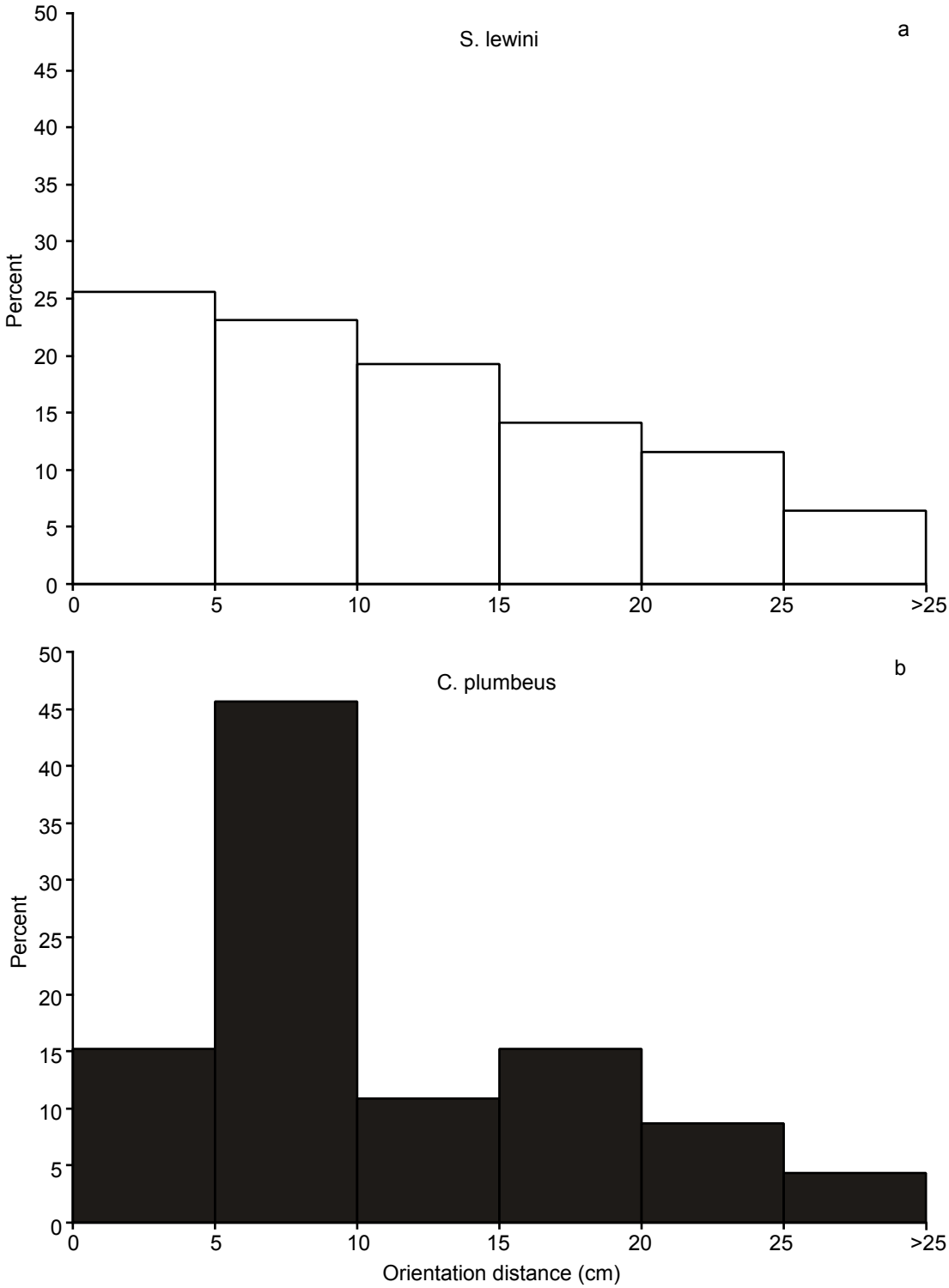

Figure 4.2 Histogram of percentage of orientations throughout the range of orientation distances. Whereas the scalloped hammerhead sharks (a) demonstrated a uniform decrease in number of orientations with increasing distance, the sandbar sharks (b) demonstrated a greater number of orientations from distances between 5 and 10cm.

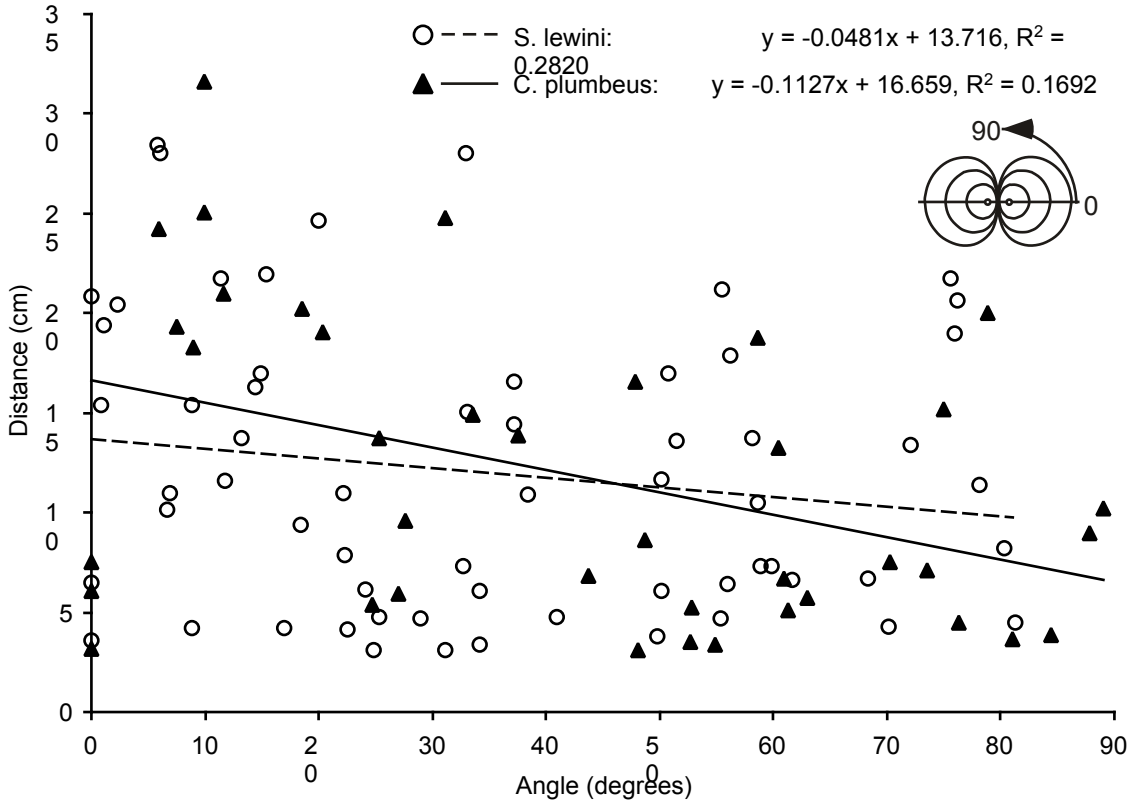

Figure 4.3 Orientation distance plotted against angle with respect to the dipole axis. Both scalloped hammerhead and sandbar sharks oriented from a significantly greater distance at smaller axis angles where the electric field strength is greatest.

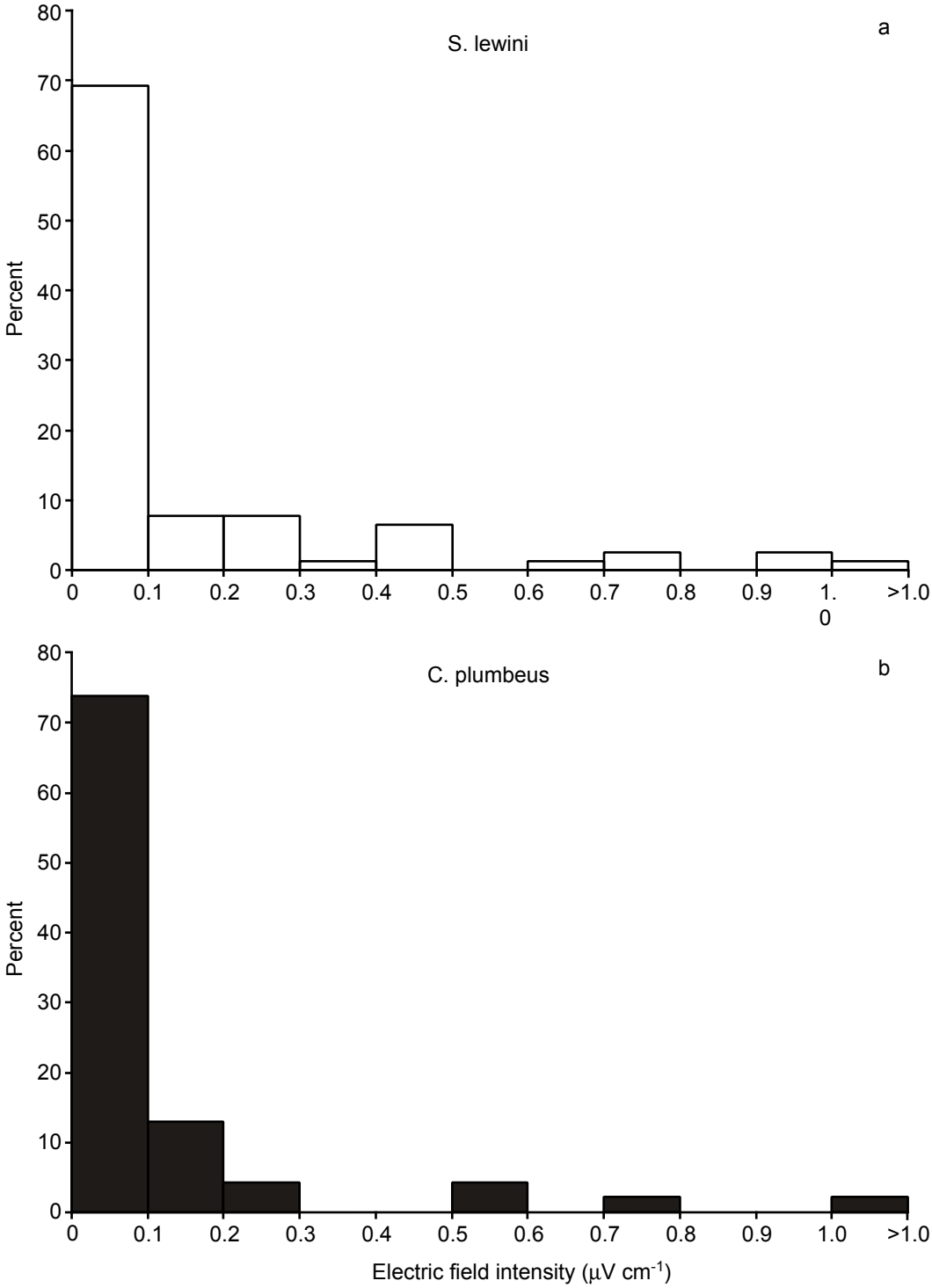

Figure 4.4 Histogram of percentage of orientations at various electric field intensities. Scalloped hammerhead (a) and sandbar sharks (b) demonstrate similar distributions across the entire range of field intensities. Approximately 70% of orientations were initiated to stimuli of <0.1 $\mu V\ cm^{-1}$ for both species with few orientations requiring a higher field intensity to initiate a response.

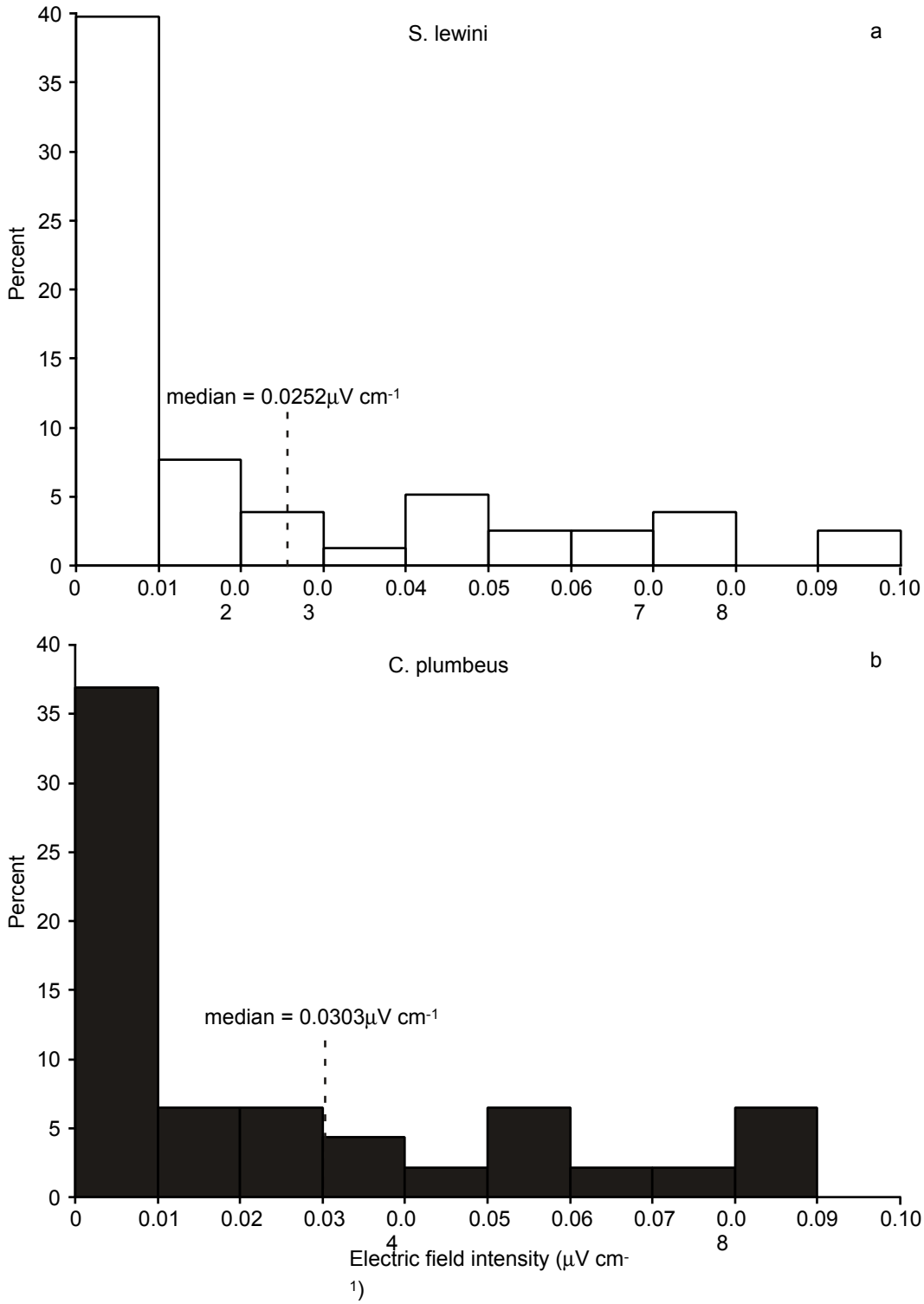

Figure 4.5 Histogram of percentage of orientations at various electric field intensities. Scalloped hammerhead (a) and sandbar sharks (b) demonstrate similar distributions across the entire range of field intensities. Both species initiated approximately 35 to 40% of orientations to stimuli of <0.01 $\mu V\ cm^{-1}$.

Orientation	Percent		Pattern
	S.lewini	C.plumbeus	
straight	33.9	37.7	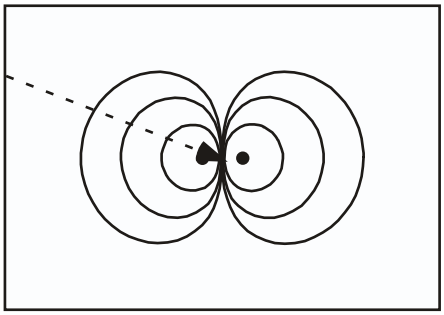
single turn	50.8	54.7	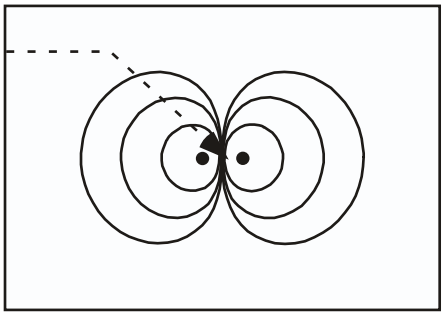
overshoot	11.3	7.5	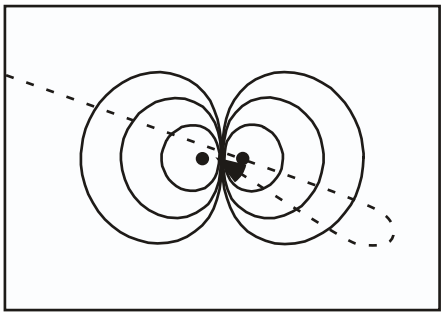
spiral tracking	4.0	0.0	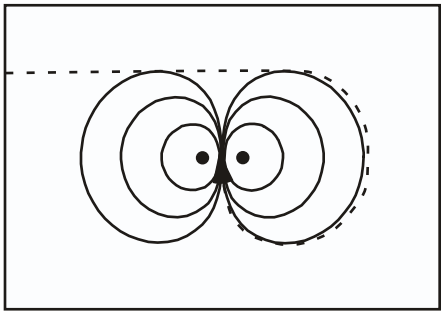

Figure 4.6 Orientation pathways demonstrated by scalloped hammerhead and sandbar sharks with frequency of occurence of each type. Solid lines indicate voltage equipotentials around the dipole and dashed lines indicate the path taken by the sharks. Whereas the hammerhead sharks demonstrated a greater variety of orientation pathways, the sandbar sharks were unable to exhibit the same repertoire of behaviors due to their stiffer body.

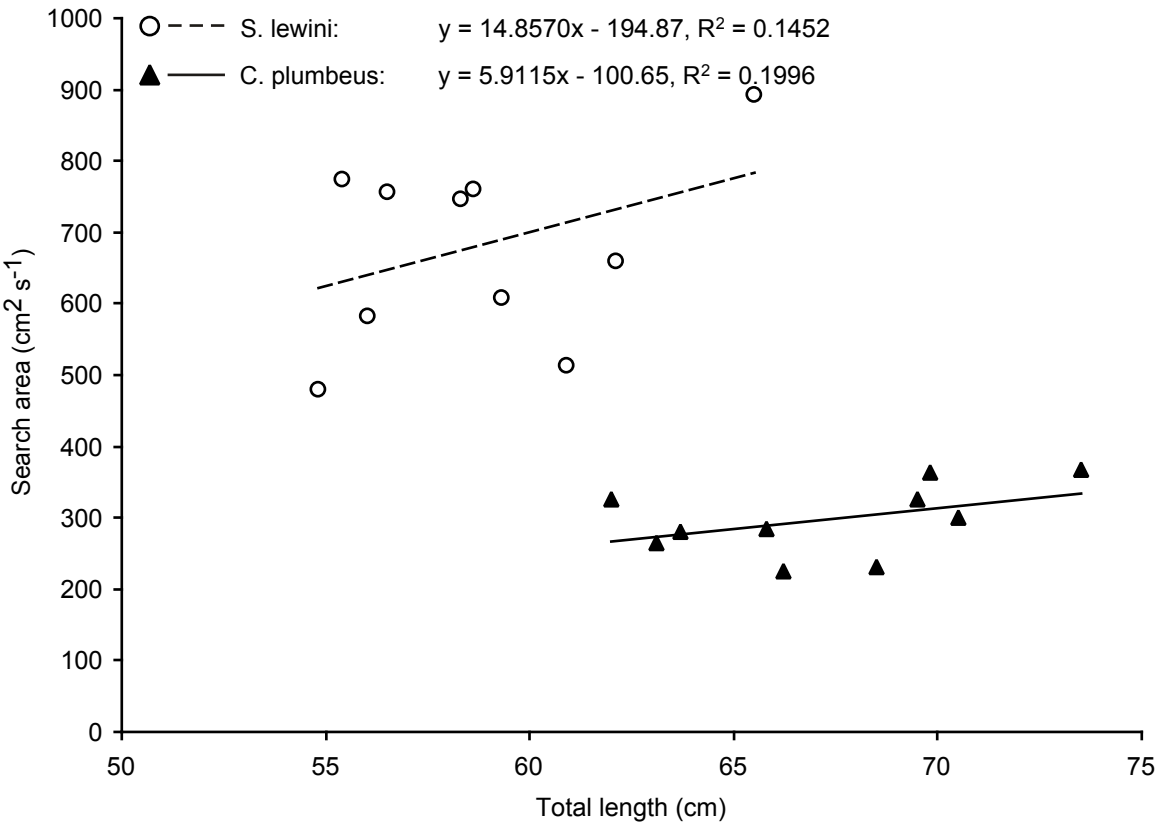

Figure 4.7 Search area sampled by the head of scalloped hammerhead and sandbar sharks. Although the regression slope was not significantly different from a flat line for either species, the search area was greater for the hammerheads compared to the sandbar sharks.

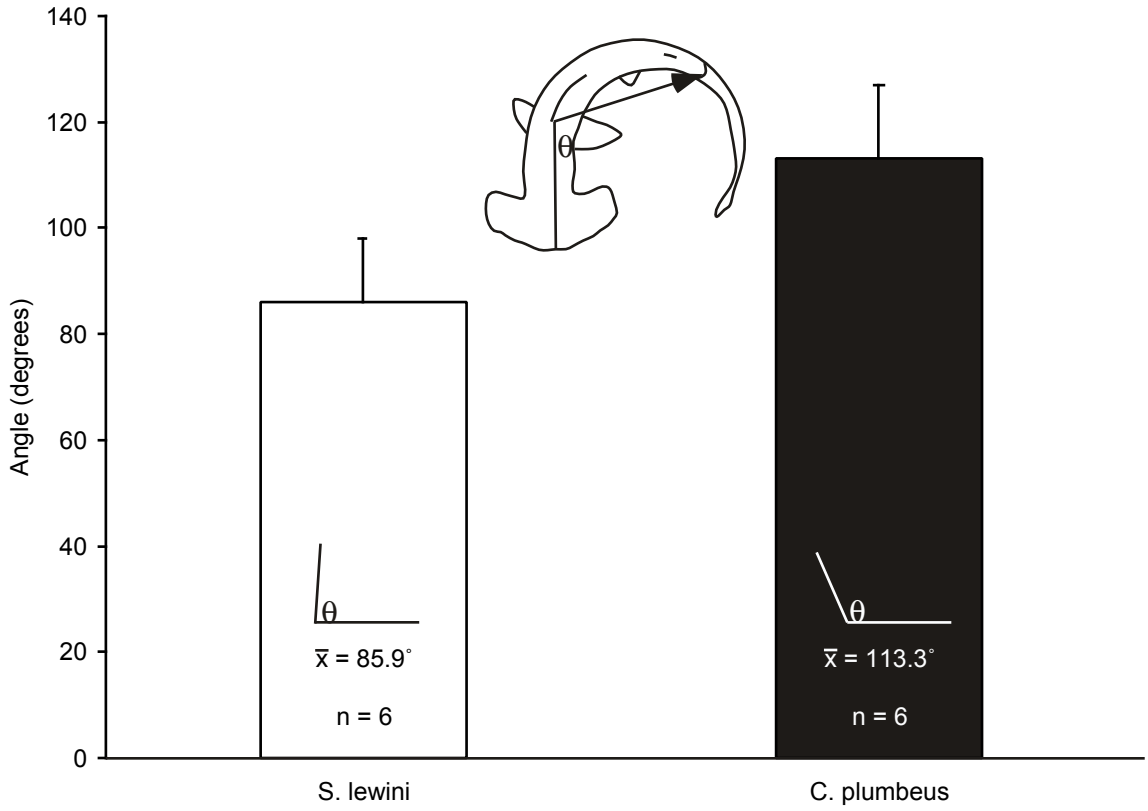

Figure 4.8 Maximum body flexure of scalloped hammerhead and sandbar sharks. Hammerhead sharks demonstrated a greater degree of flexibility with a mean maximum flexure of 85.9˚ whereas the mean maximum flexure of sandbar sharks was 113.3˚.

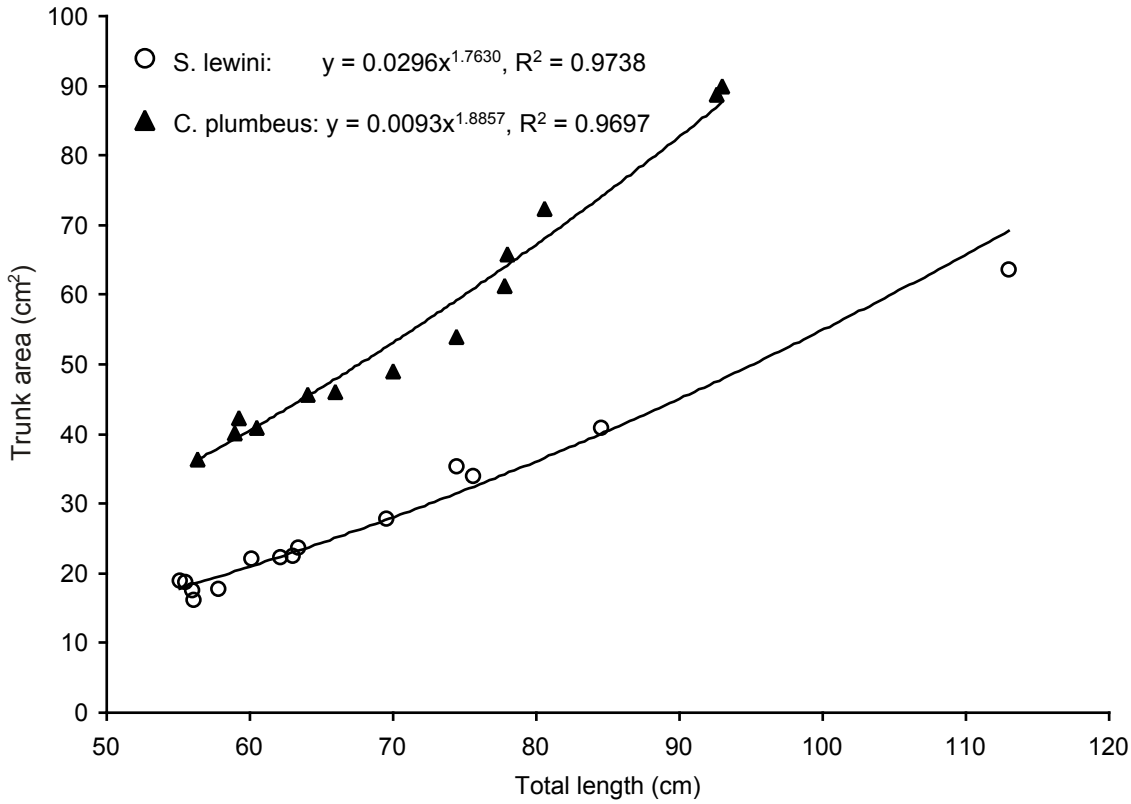

Figure 4.9 Cross sectional area of the trunk (cm^2) of scalloped hammerhead and sandbar sharks. Sandbar sharks have a significantly greater cross sectional trunk area than the hammerheads across a wide range of sizes.

CHAPTER 5

SUMMARY OF FINDINGS AND DIRECTIONS FOR FUTURE RESEARCH

SUMMARY

The evolution of the peculiar head morphology of hammerhead sharks has been the subject of much speculation. One hypothesis which has been advanced to explain the adaptive significance of the hammerhead cephalofoil is the enhanced electrosensory hypothesis. The enhanced electrosensory hypothesis states that the laterally expanded head morphology of the hammerhead sharks confers an advantage over carcharhinid sharks for detection of prey-generated bioelectric fields. This study tested the predictions of the enhanced electrosensory hypothesis by comparing carcharhinid and sphyrnid shark morphologies, behaviors and calculated sensitivities to electric dipoles.

Head morphology

The comparative head morphology of carcharhinid and sphyrnid sharks provided anatomical evidence to support the enhanced electrosensory hypothesis. Scalloped hammerhead sharks, Sphyrna lewini, possessed a head morphology that was greater in width than similar sized sandbar sharks, Carcharhinus plumbeus. The electrosensory pores were distributed over the entire surface of the head for both species and the pore distribution pattern was remarkably consistent across the sphyrnid and carcharhinid species examined. Despite the similar distribution patterns, the scalloped hammerhead sharks had a greater total number of pores than the sandbar sharks. The greater number of pores distributed over the greater surface area of the head enabled the hammerheads to

maintain the same pore density (pores cm^{-2}) as the sandbar sharks. Therefore, the ability to resolve electric fields was comparable for the sphyrnid and carcharhinid species. The hammerheads were thus able to sample a greater area with the same resolution as the sandbar sharks. The comparative morphological data thus provided support for the enhanced electrosensory hypothesis.

Response of hammerhead sharks to various electric stimuli

Taken in isolation, the morphological data are insufficient to fully address the predictions of the enhanced electrosensory hypothesis. It was necessary to devise a method to test the behavioral response of the sharks to prey-simulating electric fields. Based on the techniques of previous studies (Kalmijn 1971, 1978, 1982) a protocol was developed to quantify the response of juvenile hammerhead sharks to weak electric fields. The sharks responded as predicted and oriented from a greater distance when the dipole separation was increased. However, they did not respond from a greater distance when electric current was increased. This lack of difference in response might be attributable to the small range of tested currents. The juvenile hammerhead sharks demonstrated the greatest response to small dipoles, which likely best resembled their natural prey. Therefore, this component of the study determined that the protocol developed was adequate to elicit feeding responses and that the analysis was of sufficient resolution to detect differences in response behavior.

Comparative electrosensory abilities of hammerhead and sandbar sharks

The definitive test of the enhanced electrosensory hypothesis remained with a comparison of the sensory capabilities of carcharhinid and sphyrnid sharks. The

scalloped hammerhead sharks did not demonstrate greater sensitivity to dipole electric fields than the sandbar sharks. However, the characteristic orientation patterns for the two species differed. The hammerheads demonstrated a greater repertoire of orientation pathways which was attributable to the hydrodynamic properties of the cephalofoil as well as the greater degree of trunk flexibility. These factors enabled the hammerheads to execute more fine scale maneuvering and to initiate orientations to a target even from close range. In contrast, the greater trunk cross sectional area prevented sandbar sharks from demonstrating the same degree of flexibility.

Although the enhanced sensitivity hypothesis was not supported, the greater search area hypothesis was supported. The greater head width of the scalloped hammerhead sharks enabled them to sample a greater area per unit time than the sandbar sharks. Therefore, the wider head of sphyrnids enables them to sample a wider swath of the substratum, thus increasing the probability of encountering prey. Taken together, these components of the study demonstrate that the hammerhead sharks do have an electrosensory advantage compared to similar sized carcharhinid sharks. The primary advantage is in the greater probability of prey encounter.

Evolutionary history of the hammerhead sharks

Of the more than 380 extant shark species, only eight species are hammerhead sharks (Compagno 1999). The sphyrnids are the most recently derived of the galeoid elasmobranchs (Martin et al. 1992) and first appeared in the Miocene approximately 20 to 25 million years ago (Cappetta 1987). Two competing scenarios have been advanced to explain the evolutionary origin of the sphyrnid cephalofoil. The comparative

morphology-based hypothesis states that the sphyrnids derived from a carcharhinid ancestor, likely Scoliodon, by gradual lateral expansion of the neurocranium to form a cephalofoil (Compagno 1988). This hypothesis proposes that the basal form is found in Sphyrna tiburo, which possesses the least amount of lateral head expansion, and the derived form is found in Eusphyra blochii, in which the head width approaches one half the total length (Compagno 1984). An alternative hypothesis is based on mitochondrial DNA sequence data and states that the most extreme sphyrnid morphology, that of E. blochii, is basal and S. tiburo is derived (Martin 1993). Although this second hypothesis initially seems counterintuitive, it could be realized if one imagines a mutation in a growth regulation gene that fails to limit the growth of the neurocranium beyond its normal parameters. The resulting mutant would be an example of the "hopeful monster" (Goldschmidt 1940), and its descendants would have evolved successively less extreme head morphologies and converged toward the basal carcharhinid form from which they were originally derived. Regardless of its evolutionary history, the head morphology of the sphyrnid sharks is sufficiently adaptive to have been maintained over the past 20 to 25 million years.

Other vertebrates which independently evolved a laterally expanded head morphology include the nectridean amphibians and the cephalaspid fishes (Figure 5.1). The nectrideans were characterized by a flattened, wing-like head morphology coupled with a typical salamander-like post-cranial body. The eyes remained closely spaced in the center of the head and there were no apparent sensory structures across the width of the head (Cruickshank & Skews 1980). Thus, it is proposed that the head morphology provided a hydrodynamic function for these stream-dwelling amphibians (Cruickshank &

Skews 1980). Some cephalaspid fishes also possessed a dorso-ventrally compressed and laterally expanded head morphology. Unlike the nectrideans, the cephalaspids did have sensory structures near the distal margins of the head shield although the function of these sensory fields remains unresolved (Benton 1997). If the sensory fields were electroreceptive, the wide head of cephalaspids and hammerhead sharks might provide an example of convergent evolution.

Future research

This study examined only one hypothesis for the evolution of the sphyrnid head morphology: the enhanced electrosensory hypothesis. Several other hypotheses for the evolution of the sphyrnid cephalofoil remain to be tested. For example, it is undetermined whether the large nasal capsule of sphyrnid sharks accommodates a larger olfactory rosette compared to a carcharhinid shark. A greater olfactory epithelial surface area or density of chemoreceptors would provide an increased sensitivity to olfactory stimuli. It is also undetermined whether the wide spacing of the nostrils at the distal tips of the cephalofoil provides sphyrnids with an enhanced ability to determine directionality of a stimulus. Comparative tests of olfactory sensitivity and spatial resolution between sphyrnid and carcharhinid sharks need to be conducted to address these questions. The hydrodynamic properties of the sphyrnid cephalofoil are also largely unstudied. Although it has been hypothesized that the cephalofoil provides lift and enhances maneuverability (Compagno 1984, Nakaya 1995), this has not been empirically tested.

Additional aspects of the electroreceptive system also remain to be considered. For example, histological techniques could be employed to quantify the number of

receptor cells in the ampullae of various shark species. Receptor cell number is an important factor in increasing the signal-to-noise ratio, which helps to determine the sensitivity of a system (Raschi 1986). In addition, electrophysiological recording could be employed to measure the sensitivity of the electrosensory system as a complement to the behavioral technique used in this study. This study examined responses only to prey-simulating dipole fields but the response of various shark species to large uniform fields remains to be tested. This has implications for the shark's ability to orient within the earth's magnetic field (Kalmijn 1974, 1981). The electrosensory abilities of shark species other than carcharhinids and sphyrnids also remains largely unexplored. Therefore, many additional questions remain to be addressed in the fields of sphyrnid head morphology and elasmobranch electroreception.

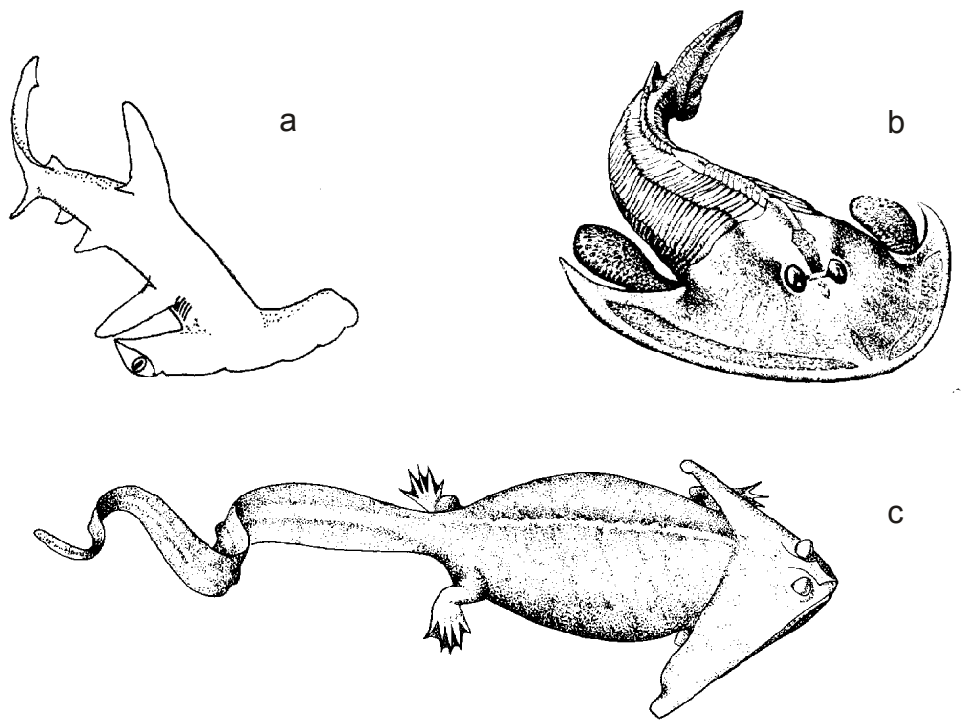

FIGURE 5.1 Illustrations of vertebrate taxa which exhibit a dorso-ventrally compressed and laterally expanded head morphology. In addition to the (a) sphyrnid sharks, a wide head morphology was also present in the extinct (b) cephalaspid fishes and (c) nectridean amphibians. (b from Benton 1997; c from Cruickshank & Skews 1980).

LITERATURE CITED

Bray, R. 1978. Night shocker: predatory behavior of the Pacific electric ray (Torpedo californica). Science. 200: 333-334.

Cappetta, H. 1987. Chondrichthyes II. Mesozoic and Cenozoic elasmobranchii. Vol. 3B Handbook of Paleoichthyology. Fischer, Stuttgart. 193 pp.

Castro, J.I. 1983. The sharks of North American waters. Texas A&M University Press, College Station. 180 pp.

Chu, Y.T. & M.C. Wen. 1979. Monograph of fishes of China (No. 2): a study of the lateral-line canal system and that of Lorenzini ampulla and tubules of elasmobranchiate fishes of China. Science and Technology Press, Shanghai. 132 pp.

Clarke, T.A. 1971. The ecology of the scalloped hammerhead shark, Sphyrna lewini, in Hawaii. Pac. Sci. 25: 133-144.

Compagno, L.J.V. 1984. FAO species catalogue, Vol. 4: Sharks of the world. An annotated and illustrated catalogue of shark species know to date, part 2: Carcharhiniformes. Food and Agriculture Organization of the United Nations, Rome, Italy. Vol. 4, Pt. 2: 251-665.

Compagno, L.J.V. 1988. Sharks of the Order Carcharhiniformes. Princeton University Press, Princeton, New Jersey. 486 pp.

Compagno, L.J.V. 1999. Systematics and body form. p. 1-42. In W.C. Hamlett (ed.) Sharks, skates, and rays; the biology of elasmobranch fishes. Johns Hopkins University Press, Baltimore. 515 pp.

Coombs, S. & R.A. Conley. 1997. Dipole source localization by mottled sculpin. I. Approach patterns. J. Comp. Physiol. A. 180: 387-399.

Cortes, E., C.A. Manire & R.E. Hueter. 1996. Diet, feeding habits, and diel feeding chronology of the bonnethead shark, Sphyrna tiburo, in southwest Florida. Bull. Mar. Sci. 58: 353-367.

Cruickshank, A.R.I. & B.W. Skews. 1980. The functional significance of nectridean tabular horns (Amphibia: Lepospondylii). Proc. R. Soc. Lond. B. 209: 513-537.

Daniels, C.I. 1967. The distribution, morphology, and innervation of the ampullae of Lorenzini in the hammerhead shark and other species. M.S. thesis, University of Hawaii. 42 pp.

Davis, E.A. and C.D. Hopkins. 1988. Behavioural analysis of electric signal localization in the electric fish, Gymnotus carapo (Gymnotiformes). Anim. Behav. 36: 1658-1671.

Gilbert, C.R. 1967. A taxonomic synopsis of the hammerhead sharks (Family Sphyrnidae). p. 69-77. In P.W. Gilbert, R.F. Mathewson, & D.P. Rall (ed.) Sharks, skates and rays. Johns Hopkins Press, Baltimore. 624 pp.

Goldschmidt, R.B. 1940. The material basis of evolution. Yale University Press, New Haven, Connecticut. 436p.

Johnson, P.B. & J.H. Teeter. 1985. Behavioral response of bonnethead sharks (Sphyrna tiburo) to controlled olfactory stimulation. Mar. Behav. Physiol. 11: 283-291.

Johnson, C.S., B.L. Scronce & M.W. McManus. 1984. Detection of DC electric dipoles in background fields by the nurse shark. J. Comp. Physiol. A. 155: 681-687.

Kajiura, S.M. 2001. Head morphology and electrosensory pore distribution of carcharhinid and sphyrnid sharks. Env. Biol. Fish. 61: 125-133.

Kalmijn, A.J. 1966. Electro-perception in sharks and rays. Nature. 212: 1232-1233.

Kalmijn, A.J. 1971. The electric sense of sharks and rays. J. Exp. Biol. 55: 371-383.

Kalmijn, A.J. 1972. Bioelectric fields in sea water and the function of the ampullae of Lorenzini in elasmobranch fishes. Scripps Institution of Oceanography Reference Series, Contribution no. 72-83. 21 pp.

Kalmijn, A.J. 1974. The detection of electric fields from inanimate and animate sources other than electric organs. p. 147-200. In A. Fessard (ed.) Handbook of sensory physiology, vol. 3: Electroreceptors and other specialized receptors in lower vertebrates. Springer-Verlag, Berlin. 333 pp.

Kalmijn, A.J. 1978. Electric and magnetic sensory world of sharks, skates, and rays. p. 507-528. In E.S. Hodgson & R.F. Mathewson (ed.) Sensory biology of sharks, skates, and rays. Government Printing Office, Washington DC. 666 pp.

Kalmijn, A.J. 1981. Biophysics of geomagnetic field detection. IEEE Transactions on Magnetics. 17: 1113-1124.

Kalmijn, A.J. 1982. Electric and magnetic field detection in elasmobranch fishes. Science. 218: 916-918.

Kalmijn, A.J. 1988. Detection of weak electric fields. pp. 151-186. In J.Atema, R.R. Fay, A.N. Popper & W.N. Tavolga (ed.) Sensory biology of aquatic animals. Springer-Verlag, New York. 936 pp.

Kalmijn, A.J. 1997. Electric and near-field acoustic detection, a comparative study. Acta Physiol. Scand. 161, Suppl 638: 25-38.

Klimley, A.P. 1993. Highly directional swimming by scalloped hammerhead sharks, Sphyrna lewini, and subsurface irradiance, temperature, bathymetry, and geomagnetic field. Marine Biology 117: 1-22.

Lowenstein, W.R. & N. Ishiko. 1962. Sodium chloride sensitivity and electrochemical effects in a Lorenzinian ampulla. Nature. 188: 1034-1035.

Martin, A.P. 1993. Hammerhead shark origins. Nature. 364: 494.

Martin, A.P., G.J.P. Naylor & S.R. Palumbi. 1992. Rates of mitochondrial DNA evolution in sharks are slow compared to mammals. Nature. 357: 153-155.

Medved, R.J., C.E. Stillwell & J.J. Casey. 1985. Stomach contents of young sandbar sharks, Carcharhinus plumbeus, in Chincoteague Bay, Virginia. Fishery Bulletin, US. 83: 395-402.

Murray, R.W. 1960. Electrical sensitivity of the ampullae of Lorenzini. Nature. 187: 957.

Murray, R.W. 1974. The ampullae of Lorenzini. pp. 125-145. In A. Fessard (ed.) Handbook of sensory physiology, vol. 3: Electroreceptors and other specialized receptors in lower vertebrates. Springer-Verlag, Berlin. 333 pp.

Murray, R.W. & W.T.W. Potts. 1961. The composition of the endolymph, perilymph and other body fluids of elasmobranchs. Comp. Biochem. Physiol. 2: 65-75.

Nakaya, K. 1995. Hydrodynamic function of the head in the hammerhead sharks (Elasmobranchii: Sphyrnidae). Copeia. 1995: 330-336.

Naylor, G.J.P. 1992. The phylogenetic relationships among requiem and hammerhead sharks: inferring phylogeny when thousands of equally most parsimonious trees result. Cladistics. 8: 295-318.

Obara, S. & M.V.L. Bennett. 1972. Mode of operation of ampullae of Lorenzini of the skate, Raja. J. Gen. Physiol. 60: 534-557.

Parker, G.H. 1909. The influence of the eyes and ears and other allied sense organs on the movement of Mustelus canis. Bull. U.S. Bur. Fish. 29:43-58.

Paulin, M.G. 1995. Electroreception and the compass sense of sharks. J. theor. biol. 174: 325-339.

Raschi, W.G. 1978. Notes on the gross functional morphology of the ampullary system in two similar species of skates, Raja erinacea and R. ocellata. Copeia. 1978: 48-53.

Raschi, W.G. 1984. Anatomical observations on the Ampullae of Lorenzini from selected skates and galeoid sharks of the Western North Atlantic. PhD dissertation, College of William and Mary. 116 pp.

Raschi, W.G. 1986. A morphological analysis of the ampullae of Lorenzini in selected skates (Pisces, Rajoidea). J. Morph. 189: 225-247.

Sand, A. 1938. The function of the ampullae of Lorenzini, with some observations on the effect of temperature on sensory rhythms. Proc. R. Soc. Lond. B. 125: 524-553.

Schluger, J.H. & C.D. Hopkins. 1987. Electric fish approach stationary signal sources by following electric current lines. J. Exp. Biol. 130: 359-367.

Sisneros, J.A., T.C. Tricas & C.A. Luer. 1998. Response properties and biological function of the skate electrosensory system during ontogeny. J. Comp. Physiol. A. 183: 87-99.

Smith, H.S. 1985. The illustrated guide to aerodynamics. TAB Books Inc., Blue Ridge Summit. 227 pp.

Sokal, R.R. & F.J. Rohlf. 1981. Biometry 2nd ed. W.H. Freeman & Co., New York. 859 pp.

Strong, W.R., F.F. Snelson Jr. & S.H. Gruber. 1990. Hammerhead shark predation on stingrays: an observation of prey handling by Sphyrna mokarran. Copeia. 1990: 836-840.

Tester, A.L. 1963. Olfaction, gustation and the common chemical sense in sharks. p. 255-285. In P.W. Gilbert (ed.) Sharks and survival. D.C. Heath and Company, Boston. 578 pp.

Thomson, K.S. & D.E. Simanek. 1977. Body form and locomotion in sharks. Amer. Zool. 1977: 343-354.

Tricas, T.C. 1982. Bioelectric-mediated predation by swell sharks, Cephaloscyllium ventriosum. Copeia. 1982: 948-952.

Tricas, T.C. 2001. The neuroecology of the elasmobranch electrosensory world: why peripheral morphology shapes behavior. Env. Biol. Fish. 60: 77-92.

Tricas, T.C. & J.E. McCosker. 1984. Predatory behavior of the white shark, Carcharodon carcharias, and notes on its biology. Proc. Calif. Acad. Sci. 43: 221-238.

Tricas, T.C., S.W. Michael & J.A. Sisneros. 1995. Electrosensory optimization to conspecific phasic signals for mating. Neuroscience letters. 202: 129-132.

Tricas, T.C. & J.G. New. 1998. Sensitivity and response dynamics of electrosensory primary afferent neurons to near threshold fields in the round stingray. J. Comp. Physiol. A. 182: 89-101.

Waltman, B. 1966. Electrical properties and fine structure of the ampullary canals of Lorenzini. Acta physiol. Scand. 66, suppl. 264: 1-60.